FACULTY OF INFORMATION TECHNOLOGY AND ELECTRICAL ENGINEERING

DEGREE PROGRAMME IN WIRELESS COMMUNICATIONS ENGINEERING

MASTER'S THESIS

LIDAR AIDED SIMULATION PIPELINE FOR WIRELESS COMMUNICATION IN VEHICULAR TRAFFIC SCENARIOS

Author	Uvindu Kopiyawattage
Supervisor	Prof. Premanandana Rajatheva
Second Examiner	Dr. Pekka Pirinen

June 2023

Kopiyawattage, Uvindu (2023) LiDAR aided Simulation Pipeline for Wireless Communication in Vehicular Traffic Scenarios. University of Oulu, Faculty of Information Technology and Electrical Engineering, Degree Programme in Wireless Communications Engineering. Master's Thesis, 53 p.

ABSTRACT

Integrated Sensing and Communication (ISAC) is a modern technology under development for Sixth Generation (6G) systems. This thesis focuses on creating a simulation pipeline for dynamic vehicular traffic scenarios and a novel approach to reducing wireless communication overhead with a Light Detection and Ranging (LiDAR) based system. The simulation pipeline can be used to generate data sets for numerous problems. Additionally, the developed error model for vehicle detection algorithms can be used to identify LiDAR performance with respect to different parameters like LiDAR height, range, and laser point density. LiDAR behavior on traffic environment is provided as part of the results in this study. A periodic beam index map is developed by capturing antenna azimuth and elevation angles, which denote maximum Reference Signal Receive Power (RSRP) for a simulated receiver grid on the road and classifying areas using Support Vector Machine (SVM) algorithm to reduce the number of Synchronization Signal Blocks (SSBs) that are needed to be sent in Vehicle to Infrastructure (V2I) communication. This approach effectively reduces the wireless communication overhead in V2I communication.

Key words: 6G, Multiple Input Multiple Output (MIMO), Light Detection and Ranging (LiDAR), Beamforming, Simulation pipeline, Integrated Sensing and Communication (ISAC), Vehicle detection, Signal to Noise Ratio (SNR)

TABLE OF CONTENTS

FOREWORD

This thesis, titled as “LiDAR aided Simulation Pipeline for Wireless Communication in Vehicular Traffic Scenarios” is an original study performed by me and submitted to the master’s degree in Wireless Communication Engineering at the University of Oulu. The research described here was carried out at the University of Oulu's Centre for Wireless Communication Engineering, primarily under the supervision of Prof. Premanandana Rajatheva with the collaboration of Nokia Standards under the project called "VASABA". The project's goal is to analyze and improve the sensing aided communication methods using sensing agents like LiDAR and camera.

I would like to express my gratitude to my main supervisor, Prof. Premanandana Rajatheva, for the support and guidance given throughout this research. Moreover, I am grateful to Nokia Standards and Centre of Wireless Communication for providing funding as well as resources to continue with this research and Dr. Pekka Pirinen for reviewing my work as the second reviewer. Additionally, I would like to express my gratitude to the members in VASABA project for the continuous guidance and support, including Sami Hakola, Timo Koskela, Oskari Tervo, Juha Karjalainen and Jari Hulkkonen in Nokia Standards. Moreover, I would like to thank all of the lecturers at the University of Oulu, as well as my parents and colleagues, for their encouragement and support throughout my whole academic period, including this research.

Oulu, June 2023

Uvindu Kopiyawattage

LIST OF ABBREVIATIONS

3GPP	3rd Generation Partnership Project
5G	5th Generation
6G	6th Generation
AI	Artificial Intelligence
API	Application Programming Interface
AR	Augmented Reality
B5G	Beyond 5th Generation
BS	Base Station
CNN	Convolutional Neural Network
CSI	Channel State Information
csv	comma separated version
DARPA	Defense Advanced Research Projects Agency
DBSCAN	Density-based Spatial Clustering of Applications with Noise
DFRC	Dual-functional Radar-Communications
DL	Deep Learning
DoF	Degree of Freedom
EKF	Extended Kalman Filter
FCD	Floating Car Data
FN	False Negative
FP	False Positive
GPS	Global Positioning System
HCI	Human Computer Interaction
IoT	Internet of Things
IRS	Intelligent Reflecting Surface
ISAC	Integrated Sensing and communication
JCR	Joint Communication and Radar
KPI	Key Performance Indicator
LiDAR	Light Detection and Ranging
LLM	Large Language Models
LoS	Line of Sight
MIMO	Multiple Input Multiple Output
ML	Machine Learning
NR	New Radio
PHY	Physical Layer
PSK	Phase Shift Keying
QoS	Quality of Service
RADAR	Radio Detecting and Ranging
RadCom	Radar-Communications
RANSAC	Random Sample Consensus
RCC	Radar-Communication Coexistence
RSRP	Reference Signal Receive Power
RSU	Roadside Unit
SaaS	Sensing as a Service
SSB	Synchronization Signal Block
SSPARC	Shared Spectrum Access for Radar and Communications
SUMO	Simulation of Urban Mobility

SVM	Support Vector Machine
TN	True Negative
TP	True Positive
UAV	Unmanned Aerial Vehicle
UE	User Equipment
URA	Uniform Rectangular Array
V2I	Vehicle to Infrastructure
V2N	Vehicle to Network
V2P	Vehicle to Pedestrian
V2V	Vehicle to Vehicle
V2X	Vehicle to Everything
VR	Virtual Reality

1 INTRODUCTION

Integrated Sensing and communication (ISAC) [1] will go beyond classical communication methodology and provide a sensing functionality to measure or even fully map the surrounding environment with details for a particular instance. With the use of ISAC technology general wireless network turns into a sensing-assisted network. There are two ways of ISAC, i.e., sensing-assisted communication and communication-assisted sensing. Within this study, we consider sensing-assisted communication enabled by LiDAR sensors. Given the increase in data-based solutions for communication, new networks are integrated with sensors such as Light Detection and Ranging (LiDAR), RGB cameras, and depth cameras to gather a large amount of data while enhancing the reliability, efficiency, and security of the network. For example, cellular networks become ubiquitously set up large-scale sensor networks, known as perceptive network [2] with this added sensor network. This generation of data can be used to improve the physical layer (PHY) optimizations, network management, and self-organization through Machine Learning (ML) and Deep Learning (DL) technologies [3],[4].

One crucial area of ISAC is sensing assisted communication. This area is currently under research to optimize the performance of future communication networks. Applications like smart cities, connected vehicles, and remote health care require high-quality wireless connectivity with high accuracy and robust sensing. The advantage of sensing assisted communication comes from not only from the possibility of easily integrating it to an existing communication system but also from effectively improving communication performance with the sensed location data. In recent past, due to this technology the roadside units (RSUs) including mainly base station (BS) are integrated with sensors and continue to add more sensing parts in the current communication infrastructure. Therefore, relevant research related to sensing assisted communication has been popular. For example, a method on two staged hybrid beamforming technique with the help of measured location information of Unmanned Aerial Vehicles (UAVs) was proposed in [5]. Liu et al. [6] used Radio Detecting and Ranging (RADAR) technology as the assisted sensor for communication. Positional data was adopted to predict the vehicle positions using Extended Kalman Filter (EKF). They provided a power allocation method which based on the location information to have pencil like beamforming.

Vehicle-to-Everything (V2X) communications are anticipated to have a significant role in next-generation wireless networks, facilitating various promising applications. These applications include autonomous driving, traffic management, intelligent transportation, and more. In addition to achieving high Quality of Service (QoS), the environment sensing capability of vehicles is crucial in V2X networks. This is particularly important in scenarios with high vehicle density and mobility, where stringent requirements for positioning accuracy and latency exist. With the already integrated Global Positioning System (GPS) or local proximity sensors of the vehicle, there is an error margin of around 10 meters, which can become much worse in some practical situations like in traffic. Moreover, GPS positioning might not be available or suffers from severe interference in some rural areas. Therefore, the use of more position detection sensors is needed to enhance V2X communication without having any sensor local movements and with low detection error margin.

Sometimes it is not practical to build these large sensors aided networks just to test novel research ideas related to ISAC. That's where the simulation environment comes into the play. Simulating environments for sensing assisted communication hold immense potential in advancing the development and optimization of this emerging field. By providing a virtual platform that mimics real-world scenarios, simulation environments enable researchers and

practitioners to test and evaluate various aspects of sensing assisted communication systems in a controlled and repeatable manner. Such simulation environments offer several benefits, including cost-effectiveness, scalability, and the ability to simulate a wide range of scenarios that may be challenging to replicate in physical deployments. In Chapter 2 under Simulation frameworks for wireless communication explains more about how sensing assisted communication will benefit from simulation frameworks, more specifically for vehicular communication networks.

With the created virtual simulation for vehicular traffic, it is possible to have advances in multiple areas related to vehicular communication such as beamforming, blockage prediction, channel planning, improved Line of Sight (LoS) handover, etc.

Millimeter waves and Massive Multiple Input Multiple Output (MIMO) are significant technologies for wireless systems. They enable high data rates and multiplexing gains through directing radiating pattern created by antenna array, which is the beam towards user equipment (UE). This process is known as beamforming. Moreover, massive MIMO systems are capable of mitigating interference and providing robust performance in challenging propagation environments. The research in massive MIMO includes adapting the technology to different scenarios such as vehicular environment and the question of sensing assisted beamforming. This is also known as intelligent beamforming where positional data is processed through learning algorithms to have higher throughput and data rates. This is explained more in Section 2.3.

This thesis provides a simulation pipeline with the aforementioned technologies for a vehicular traffic scenario and gives a solution to reduce the wireless overhead in MIMO beamforming with the acquired data from the pipeline.

1.1 Background and motivation

In recent past, there have been large number of elements added to the wireless networks and it becomes more complicated. With the development of MIMO, the adoption of large number of antenna arrays in both transmitter and receiver side has turned into a necessary item in order to cope up with current QoS, throughput and data rate of wireless systems. Also, one challenge is coordination overhead associated with large channel matrices generated by MIMO antennas.

Moreover, with the development of ISAC [1] technology sensors have been added to the wireless systems. This added technology affected wireless systems to have high capital and maintenance cost. Even though this increase of complexity in wireless systems affected all types of communication systems, the impact on vehicular communication is large [7]. V2X communication has to struggle with high mobility scenarios like traffic junctions in an urban area. In highly populated areas like in city environment, V2X communication will have different interferences. Managing interference and ensuring coexistence with multiple systems is a significant challenge, which requires additional computational complexity. Vehicular networks involve a large number of vehicles communicating simultaneously. The wireless communication system should be scalable to support a growing number of vehicles without compromising performance. To achieve this scalability with these added elements and network complexity has become difficult. Also, ML and DL techniques are used for most parts in wireless communication including channel modelling, spectrum management, resource allocation, network security, beamforming in MIMO systems, Intelligence of Things (IoT), etc.

Nevertheless, to handle the wireless network complexity and perform studies and research related to ML and DL tasks, researchers need a simulation environment and data sets that they

can easily change according to their objectives. Also, current research on ML applications to 5G focuses on how utilization of data obtained directly from sensors like LiDAR and cameras can enhance the efficiency of communication in distinct levels of the communication system [8], [9], [10]. But the possibility of having physics engines, realistic 3D models, and algorithm deployment environments to test current communication systems virtually helps in terms of Artificial Intelligence (AI) applications in 6G and beyond.

1.2 Research problem

Physical layer optimization in wireless communication systems using ML and DL is currently under study for future communication networks. 6G systems are expected to support augmented reality, high-fidelity holograms and multi-sensory communication [11]. From the above-mentioned applications, using sensor data to improve wireless systems has become a separate research area. In vehicular traffic communication with high mobility environment, it is important to identify the positioning information of UEs and vehicles to reduce the wireless communication overhead.

But most of the current infrastructures do not yet support sensors like LiDAR due to the high capital cost. Additionally, the full potential of LiDAR in communication systems has not yet been fully realized, and there is ongoing research focused on exploring the possibilities and advancements that can be achieved by integrating LiDAR technology into communication systems. Therefore, it is necessary to have a simulation pipeline where researchers can control and get required datasets for further studies. There is little research related to that area, specifically in vehicular traffic scenarios with LiDAR data [12], [13].

Also, the behavior of LiDAR as a RSU in vehicular traffic scenarios is not addressed in most research. The majority of studies related to V2X communication involving LiDAR focuses on its installation on vehicles, primarily for the purpose of autonomous navigation and perception tasks but not for communication perspective. Therefore, in addition to the simulation pipeline another aspect is to identify LiDAR performance as a RSU in V2I communication with respect to different parameters like LiDAR height, range, laser point density, etc., and how it can be used to reduce the wireless communication overhead. More specifically another considered research problem is how to increase Reference Signal Receive Power (RSRP) for high mobility UEs inside the vehicles with the LiDAR sensor data.

1.3 Selected scope

When it comes to ISAC technology there are several research areas to consider, including different ISAC applications, performance tradeoffs, waveform design, receive signal processing, sensing assisted communication and communication assisted sensing. From the above sections tradeoffs study and signal processing parts are related to the integration gain while communication assisted and sensing assisted communication is related to the coordination gain that added from ISAC.

There are multiple applications where the mentioned research areas can be used. For example, to provide a sensing as a service, smart home, V2X network, industrial manufacturing, remote sensing, environmental monitoring and human computer interaction (HCI). These applications can improve using all main research areas that mentioned previously, but in this

thesis the target is to concentrate on how to improve V2X communication with the sensing assisted element.

Going further deep into the scope, from V2X communication we selected one sub part of it called Vehicle to Infrastructure (V2I) communication. There are multiple sensors that can be used to enhance the V2I communication, but in this study a more specific focus area will be using LiDAR as the sensing agent.

One aspect of research related to LiDAR assisted V2I communication is the ability to represent the environment with all BSs, sensors, moving vehicles, site specific details such as buildings, roads, trees, etc., as a virtual model. Hence, this study specifically focuses on developing a simulation framework for LiDAR aided vehicular traffic scenarios and how the LiDAR performance will affect on vehicle detection in high mobility environment with respect to different controlled parameters (as mentioned in Section 1.2 Research problem) of the sensor.

With the developed virtual framework there are possibilities to do research and simulate environments on fields like MIMO beamforming, blockage prediction, LoS handover, channel planning and prediction, etc. MIMO beamforming is selected for this study, to research how LiDAR assisted beamforming helps to reduce wireless overhead of V2I communication.

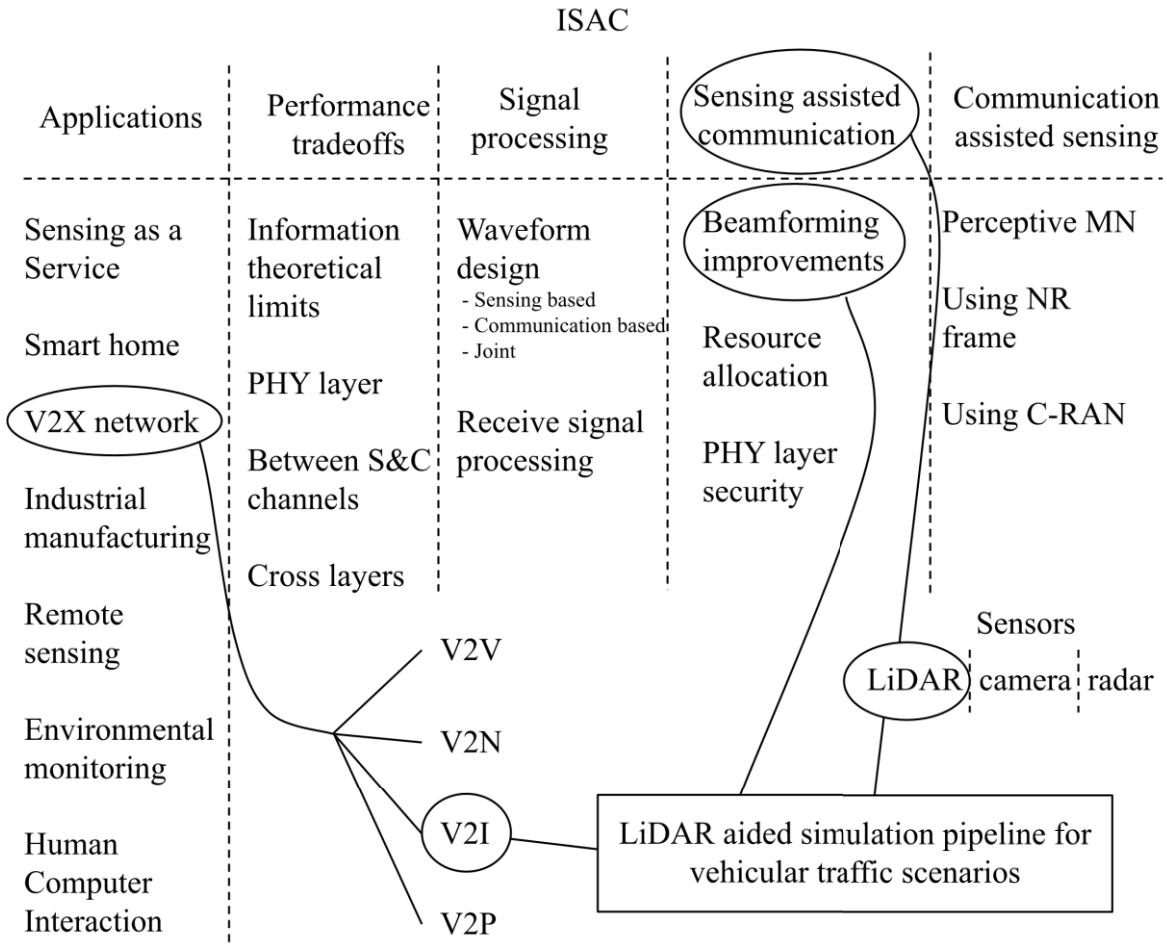

Figure 1: Graphical representation of scope of the study.

1.4 Contribution

There are mainly two contribution parts from this study,

- Simulation pipeline is developed to provide controllable simulation framework and analyze how LiDAR performs as a RSU in vehicular traffic scenarios. It includes integration of publicly available real map data into a physics generator to simulate and output vehicle location details, then fuse those physics generated data into a 3D dynamic simulation through a developed transition algorithm, testing a geometric feature-based vehicle detection algorithm in LiDAR incorporated vehicular traffic environment, use of custom develops error model to identify LiDAR behavior against different controllable parameters in the user space. Conclusions of LiDAR characteristics in vehicular traffic scenario are taken by analyzing generated graphs from the custom error model.

- A novel periodic beam index map to reduce wireless communication overhead and to reduce the number of SSBs needed in vehicular communication. This is deployed to increase the RSRP of high mobility UEs inside vehicles using LiDAR as a sensing agent.

1.5 Organization of the Thesis

This thesis comprises a total of five chapters. Chapter 1 provides a descriptive introduction about the selected research including main introduction to the research study, motivation, specific problem trying to address in this thesis, scope of the study and contribution. In Chapter 2 an extensive literature review is conducted to evaluate the ISAC technology, the added advantage of using sensing assisted communication in vehicular networks and some applications of ISAC. Moreover, the comparison of sensors to use in sensing assisted environment is evaluated through literature and provided the reasoning behind selecting LiDAR as the main sensing agent for the vehicular networks. Then the basics of MIMO beamforming and literature on intelligent beamforming is presented. As for the final part of Chapter 2, comparisons between currently available datasets and simulation frameworks are discussed. Chapter 3 shows the methodology of proposed solution, which consists of developed simulation pipeline with custom error model and precoder based beamforming calculation. Chapter 4 contains results and discussion of outputs from the simulation pipeline and a thorough analysis of LiDAR characteristics in a vehicular traffic scenario with quantitative results. Furthermore, Chapter 4 presents a novel approach of reducing wireless overhead using a method called periodic beam index map. Precoder based beamforming calculation mentioned in Chapter 3 is used to develop this novel approach and results are presented. Finally, a detailed conclusion to the thesis with potential future work is provided in Chapter 5.

2 LITERATURE REVIEW

2.1 Integrated Sensing and Communication

ISAC, which stands for Integrated Sensing and Communication, is a design paradigm that focuses on optimizing the utilization of limited wireless and hardware resources while fostering mutual benefits through the integration of sensing and communication systems. This paradigm encompasses various enabling technologies that facilitate this integration. To explain further, sensing and communication operations, which involve collecting information from noisy observations and transferring tailored signals in a noisy environment, respectively, are traditionally treated as separate tasks. However, the main goal of ISAC is to add the mentioned system functions and explore the trade-offs and performance improvements achievable through their integration. With the aggregate of communication and sensing part, ISAC aims to improve spectral and energy efficiencies by minimizing hardware as well as signaling costs.[1] Previously, these two functionalities competed for various resources, but ISAC seeks to overcome this competition by fostering a deeper integration paradigm. In the ISAC paradigm, the traditional view of sensing and communication as separate goals is replaced with an aggregated approach, where communication-assisted sensing and sensing-assisted communication functionalities collaborate to enhance each other's performance. These methods create a new network type called "perceptive networks" [2], where such networks sense the environment through different sensing agents and provide useful information. One example is sensing aided vehicular beamforming, which is the area that focuses as part of this thesis.

What are the benefits of using ISAC, paper [1] shows that there are core two possible gains,

1. *Integration Gain:*

   This establishes the superiority of ISAC over independent sensing and communication functionalities. Integration allows for efficient hardware utilization by coupling components and resources. This integration brings benefits such as improved hardware efficiency, reduced energy consumption, lower latency, and decreased signaling expenses. When sensing and communication functions operate within the same frequency band, communication propagation resembles radio sensing. Current signaling strategies for sensing and communication exhibit similarities, particularly in beamforming and ISAC signal waveform generation. By harmonizing these functionalities and adopting a unified waveform, wireless resources can be utilized more efficiently, leading to enhanced integration gain. Integration also enables resource sharing among sensing and communication modules, optimizing hardware utilization and reducing redundancy in components like antennas, processors, and memory. The integration of RF transceivers and ADCs has enabled the development of radar or communication System-on-Chip (SoC) solutions. This integration can be achieved through System-in-Package (SiP) chipsets, resulting in more compact and cost-effective designs while maintaining or improving overall system performance.

2. *Coordination Gain:*

   Coordination gain simply is the mutual assistance between sensing and

communication. Communication requires situational awareness of the environment and equipment. Usually, one part of this is known as Channel State Information (CSI). Additionally, considered users or interference and even representation of the surrounding environment corresponds to the situational awareness. Such kind of information can be shared in a cross function or cross user manner. Integration of hardware helps to achieve this mutual assistance. Coordination gain enables the complete utilization of design DoFs, whereas the performance of other waveforms is limited by established standards. Let's consider an example where coordination gain can be achieved. Nowadays, roadside communication units are equipped with sensors (e.g., cameras, radars) in addition to the mmWave massive MIMO systems and use that information to serving high mobility vehicles with narrow and high directional beams although there is a possibility of beam misalignment, which can potentially compromise the transmission rate of communication [14]. In such a scenario, if a frequency-independent representation of the spatial signal paths between sensor and vehicle can be acquired, it becomes possible to reuse situational information within the system to improve beam tracking. This is feasible even when the sensor and communication systems are only loosely connected or coupled. So, the coordination gained comes into the play.

There are key performance indicators that should consider when measuring the capability of ISAC technology,

Table 1. Sensing key performance indicators (KPI) in ISAC context.

KPI	**Description**
Accuracy	Difference between sensed and real values. E.g., distance, velocity, angle etc.
Coverage	Range and field of view limits within which objects can be detected by the sensor.
Resolution	Separation between multiple objects in range, angle, velocity etc.
Detection/false alarm possibilities	Possibility of detecting an object when one is present/not present.
Availability	Percentage of time for which a system can provide the sensing service according to requirements.
Refresh rate	Frequency which data from the sensor is taken.

2.1.1 Motivation for ISAC

Most upcoming and new applications in communication networks demand high QoS as well as accurate and robust sensing capability. Sensing will play a compelling part in B5G and 6G.

Radio sensing and communication network systems are undergoing continuous advancements in high frequency bands, large antenna arrays, and miniaturization. Consequently, these systems are becoming more alike in terms of their hardware architectures, channel characteristics, and signal processing techniques. The mentioned convergence presents a good ability to incorporate sensing capabilities into wireless systems. Consequently, future communication networks can transcend traditional communication functions and provide pervasive sensing services, enabling the measurement and even imaging of the surrounding environment.

The network's capability to gather sensory data from the surrounding through this integrated sensing functionality is considered a crucial element for mastering and developing smartness in the future smart world. It holds great potential for various location and environment-aware scenarios, such as V2X communication, smart homes, smart industrial manufacturing remote sensing, environmental monitoring, and human-computer interaction. These are just a few examples of the extensive range of applications where the fusion of sensing and communication can be leveraged.

Another main motivation of using sensory details is coming from the acquiring of artificial intelligence to the communication systems. In most of these use cases you need substantial amounts of data to run the learning algorithms and those data can be acquired only with a sensor infrastructure inbuilt with the communication systems.

2.1.2 History of ISAC

Despite recently gaining significant consideration from academic as well as from wireless industry, the concept of ISAC has been used by many research areas for several decades under various given names. Earlier terminologies such as Radar-Communications (RadCom) [15], Joint Communication and Radar (JCR) [16], Joint Radar and Communication (JRC) [17], and Dual-functional Radar-Communications (DFRC) [17] have been used to describe similar concepts. Although these terms may have slight nuances in meaning, the underlying sensing functionality primarily refers to sensing using radar technology, and it traditionally played a vital role in the context of ISAC.

The roots of this ISAC methodology can be moved through the early developments of radar technology. The first long range radar called "Mammut" developed by Germans during World War II [18]. The first MIMO system patent was in 1994. These developments of radar and MIMO inspired each other for the birth of ISAC. In 2013, a project called "Shared Spectrum Access for Radar and Communications (SSPARC)" led by Defense Advanced Research Projects Agency (DARPA) cause "radar-communication coexistence (RCC)" within the area of cognitive radio. It is anticipated that individual radar and communication systems will operate in the same frequency band, without causing interference to one another [19]. Additionally, degrees-of-freedom (DoFs) and antenna diversity concepts which were taken from MIMO wireless communication theory become also helpful in the process of MIMO radar [20]. The radar community presented different ISAC types, with the concept of combining information into radar waveforms. As for the first ISAC waveform design integrating chirp signals with phase-shift keying (PSK) modulation [21] becomes popular with the ISAC community.

Both radar and communication technologies have progressed in parallel, sharing common advancements. According to the communication context, utilizing high frequency bandwidth and large antenna arrays has significantly enhanced capacity of signals and facilitated the establishment of numerous connections. Conversely, expansion of bandwidth and increase the number of antennas has again had a considerable positive impact on radar performance, particularly in terms of range and angular resolutions. This means radar systems are now more capable of accurately sensing more targets or mapping complex environments. Due to these overlapping advancements, the line between radar and communication has blurred, and the traditional boundary separating the two has become less distinct. The functionality of sensing is no longer limited exclusively to radar infrastructure. Instead, wireless infrastructures and

devices are now capable of performing sensing tasks through radio emission and signaling. This convergence of capabilities forms the technical foundation and concept of ISAC [22].

2.1.3 Use cases of ISAC

This subsection covers five potential ISAC applications with examples. Use case studies are coming from [22] to further show the importance of ISAC in B5G and 6G.

1. *Enhanced localization and tracking:*

   Because to limitations like low range and angle resolution with 4G and 5G antennas cellular communication systems achieve only meter level accuracy, but with the additional sensing aspect the B5G, 6G networks can be adapted with centi-meter level accuracy, which required for more accurate use cases such as "pencil-like" MIMO beamforming etc. General position detection coverage accuracy is not enough and the positioning accuracy for outdoor is less than the indoor environment. In either case currently available wireless systems predominant approach is to attach wireless equipment such as smartphone to the object that require positioning and tracking, or in some cases computing its position using signal cooperation and geometrical relationships with other deployed wireless nodes like BSs and routers. Anyway, this device-based localization is not applicable for a large and diverse scenario. Hence, there is a requirement for add sensor agents to receive the location information directly without relying on the wireless or position-based equipment that are already in the communication system. With the addition of new sensor data coupled with Doppler processing and from multi path MIMO components, cellular networks can enhance the localization sensitivity with the comparison to current technology. This idea does not limit to just enhance the localization accuracy but also it will accumulate the total environment awareness which can be used to reduce the wireless overhead.

2. *Smart home:*

   With the development of IoT devices current home technology and functions have become automated. It is expected to have reliable and fast connection between hardware to ensure convenient, safe and comfortable lifestyle. Smart devices will become able to understand people using sensors. To perform such intelligent decisions ISAC, enable the infrastructure and architecture in the communication aspect. For example, ISAC is used to improve in the areas of health care, activity recognition, home security, etc., For going further, human activity recognition is also an advancement in smart home application. As we know wireless signals are affected by dynamic objects including human movements. This change creates phase and amplitude variations in these wireless signals, which can be used to identify human presence, falls, sleep and daily activities.

3. *Smart manufacturing and Industrial IoT:*

   Industrial automation often requires handling large networks in high interference environment. These scenarios involve robots and network nodes that are used to perform complicated and gentle assignments that need wireless connectivity in access points and with minimum latency. The integration of sensors into the communication system helps

robots and equipment to seamlessly navigate, work between access points and map the surroundings for later use. Since ISAC provides such functionalities, the signaling overhead dedicated will be reduced. Moreover, swarm navigation, platooning and imaging technologies involved in smart manufacturing process will require high reliability, low latency with multiple parallel wireless connections which are achieved through ISAC.

4. *Human Computer Interaction:*

Dynamic movements are able to extract from time, Doppler and frequency changes in the reflected signal. Hence, gesture detection becomes a popular subject, and it is shown that it can be detected using wireless technology. With the advance of signal processing with broad antenna beams, high temporal resolution can be achieved instead of high spatial resolution. These high dynamic gesture recognitions become feasible due to the addition of dedicated sensing capabilities injected to the wireless systems. One example of such a system is gesture-based touch-less interaction screen with proximity sensor.

5. *Environmental monitoring:*

Humidity, particle concentration etc. like environmental information can be extracted using wireless signals. Different frequency ranges are sensible for different changes in the environment. As an example, high frequency mmWave signals are responsive for humidity because those frequencies are much closer to water absorption bands. Processed path loss information between BS and UE provides whether there are any rainfalls or any atmospheric variations in the wireless signal transmitted area. Now consider a cellular system with built in sensors such as humidity and temperature, those can be served as real time environmental variation monitoring facilities.

Numerous research studies have delved into enhancing the performance of ISAC, focusing on optimizing both transmission throughput and sensing capabilities. For instance, one study [23] examines the basic capability aspects of ISAC models, providing insights into the attainable regions for both uplink and downlink communication rates as well as sensing rates. Another study [24] investigates an algorithm for jointly designing beamforming techniques with the aim of increasing the overall performance of sensing and communication, considering weighted objectives. In a prior work [25], they introduced an intelligent reflecting surface (IRS)-based ISAC system that operates in terahertz band to maximize system capacity. Another study [26] by Zhang et al. examined a scenario involving multiple unmanned aerial vehicles and their cooperative detection enabled by ISAC. Liu et al. [27] investigated a vertical federated edge learning system that utilizes distributed ISAC for collaborative object motion recognition. Huang et al. [28] explored ISAC-assisted mobile edge computing, incorporating an IRS to enhance mobile edge computing and radar sensing performance. As for another research effort [29], the ISAC system capitalized on millimeter wave technology to get extra precise sensing details. In [30], ISAC was associated with digital twin technology to consider the challenge of resource allocation and task scheduling in vehicular edge computing.

2.2 Sensing assisted vehicular communication

In vehicular communication, there are mainly four parts: Vehicle-to-Vehicle (V2V), Vehicle-to-Network (V2N), Vehicle-to-Infrastructure (V2I) and Vehicle-to-Pedestrian (V2P). Usually, these four areas are included in vehicle-to-everything (V2X). Vehicular communication networks have a pivotal aspect in shaping the forthcoming transportation model by enabling efficient and intelligent communication between vehicles, infrastructure, and the surrounding environment.[7] The research on enhancing vehicular communication can benefit in several areas. For example, traffic safety can be improved by the real-time transfer of critical information between infrastructure and vehicles. Such communication facilitates the implementation of advanced safety applications like cooperative collision avoidance, intersection management, and pedestrian detection. Efficient utilization of road infrastructure is a pressing concern in today's congested cities. Vehicular communication networks enable the seamless coordination of traffic flow, optimizing routes, managing congestion, and improving overall traffic efficiency. Through cooperative maneuvers, platooning, and adaptive traffic signal control, these networks can minimize delays, reduce fuel consumption, and enhance the overall throughput of transportation systems. Also, advances in vehicular communication directly benefit autonomous vehicles to navigate and receive data-driven decisions in real-time. Finally, environmental sustainability is also achieved from the above-mentioned areas by optimizing traffic flow, reducing congestion, and minimizing emissions.

Next-generation wireless networks, such as B5G and 6G, are anticipated to play a crucial role in enabling sensing-aided vehicular communication. High data rates, low latency, support of high device density, improved reliability, network slicing and enhanced positioning and localization are some of those key advantages in the vehicular communication with B5G and 6G with high mobility scenarios. Therefore, use of sensors to improve the V2X communication makes it more usable with new communication technologies.

As for the sensing, RSUs are built with LiDAR/radar systems to provide sensing as a service (SaaS). These services include obstacle detection, UE localization, remote sensing and environmental awareness through depth maps. But in those RSUs sensing and communication deployed in different hardware as separate units. Nevertheless, dedicated sensing and communication systems require significant spectrum and hardware resources. As a result, cohabiting sensing and communication functionalities into the same spectrum and hardware has emerged as a feasible solution to enhance energy, spectral and hardware efficiency. Several preliminary experiments have demonstrated that V2I networks based on ISAC can achieve highly accurate localization with an accuracy in the order of centimeters, all while maintaining satisfactory communication rates [31]. Moreover, ISAC-based V2I networks have the added advantage of conserving spectral resources and reducing hardware costs. As a result, there has been significant interest from both academic and industrial communities in researching and developing ISAC-based V2I systems [32].

Table 2. Comparison between LiDAR, camera and radar as a sensing agent for vehicular communication.

Criteria	**LiDAR**	**Camera**	**Radar**
Principle	Uses laser beams to measure distances and create 3D point clouds	Captures visual images using light sensors	Emits radio waves and measures the time for their reflection

Range	Typically, hundreds of meters	Dependent on camera type and lens; generally shorter range	Several kilometers
Accuracy	High	High (dependent on camera resolution)	Moderate
Resolution	High spatial resolution, low angular resolution	High spatial resolution, high angular resolution	Low spatial resolution, high angular resolution
Robustness in different environmental conditions	Works well in various lighting conditions and weather (except heavy fog or rain)	Highly dependent on lighting conditions; affected by darkness, glare, etc.	Works well in all weather conditions (except heavy precipitation)
Privacy	Less privacy concern due to the type of data (depth information) being collected from the sensor	Privacy concerns is high because cameras collect visual data	Less privacy concern due to radio wave emission.
Cost	Relatively expensive	Low	Moderate to high
Complexity	Directly provide the point cloud data but additional processing is needed	Image processing is applied withing the sensor to provide usable visual data	Need external processing
Limitations	Affected by adverse weather conditions and highly reflective surfaces	Affected by adverse weather conditions and cannot even operate without light.	Difficulties with distinguishing between close objects, limited object identification capabilities

According to Table 2, it is clear that the most suitable sensing agent for vehicular networks is the LiDAR.

2.3 Intelligent beamforming

What is MIMO beamforming?

The utilization of multiple antenna elements at the transmitter and receiver can be employed to achieve diversity gain rather than capacity gain. In this approach, the same symbol, multiplied by a complex scale factor, is transmitted over each transmit antenna, resulting in an input covariance matrix with unit rank. This technique is commonly known as MIMO beamforming. The symbol x is transmitted over the i^{th} antenna with weight v_i, while on the receiving end, the signal received on the i^{th} antenna is multiplied by u_i.

To ensure consistency, both transmit and receive weight vectors are normalized to achieve the magnitude of 1, such that resulting signal is,

$$y = \boldsymbol{u}^* \boldsymbol{H} \boldsymbol{v} x + \boldsymbol{u}^* n \tag{2.1}$$

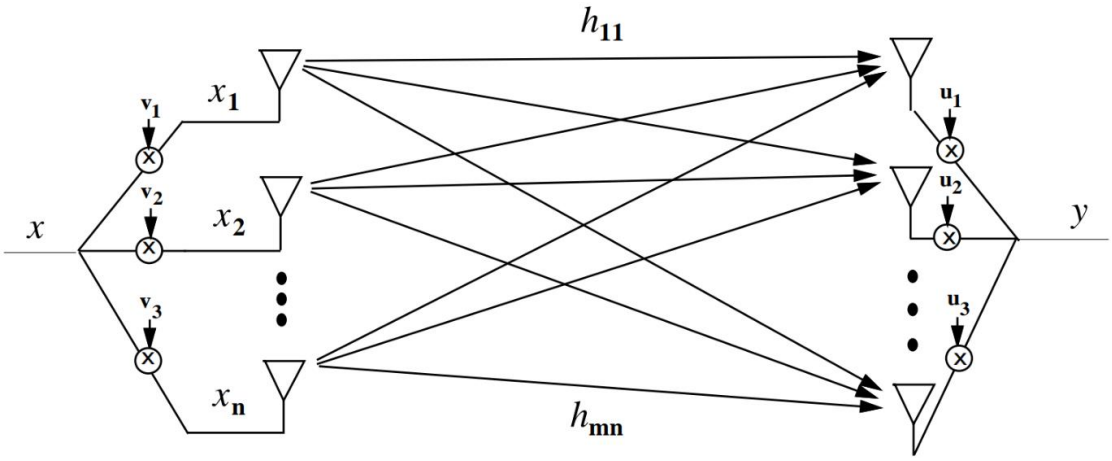

Figure 2. MIMO beamforming channel.

where $\boldsymbol{H}$ is the channel matrix, n has i.i.d. noise parts. Due to coherent combining of multiple signal paths, beamforming technology provides diversity gain. CSI at the receiver is usually expected since it's need for coherent combining. Then the diversity gained relies on whether the CSI is available at the transmitter.

The optimization of the received SNR is achieved by selecting the principal left singular vector $\boldsymbol{u}$ and the principal right singular vector $\boldsymbol{v}$ of the channel matrix $\boldsymbol{H}$, given that $\boldsymbol{H}$ is known. By choosing these singular vectors, the received SNR is maximized, leading to improved signal quality and enhanced communication performance. In cases where the channel is not known at transmitter, the transmit antenna weights are set to be equal. However, the absence of transmitter CSI leads to a lower SNR and capacity compared to scenarios where optimal transmit weighting.

Intelligent beamforming and smart antenna solutions play a crucial role in ensuring optimal performance, stable throughput, reduced interference sensitivity, extended coverage, support for highly mobile applications, and energy efficiency at the physical level. Over time, antenna technologies have evolved from basic and passive antennas to more advanced active antennas that incorporate increasing levels of intelligence to leverage environmental knowledge and optimize radio connections. This evolution has already been integrated into 5G communications and will be further enhanced by the emergence of 6G communications, where all elements within the communication chain will possess some degree of intelligence or the ability to operate optimally with training. At this level, ML, particularly deep learning, can provide an ideal solution for enabling adaptive and real-time massive MIMO beamforming. ML can help capture structural information of radio channels by following mobility patterns, coordinate beams with neighboring base stations, allocate power efficiently, adapt emission patterns for mobile devices, and utilize beamforming for value-added services. Employing dedicated hardware alongside dedicated algorithms can facilitate the implementation of efficient machine learning solutions, supporting a new generation of intelligent beamforming and smart antennas [33].

One such example of intelligent beamforming is Chang Liu et. al learning based predictive beamforming technology for V2I communication [34]. In ISAC point of view perspective, an efficient beamforming design is crucial. However, its effectiveness heavily relies on accurate channel tracking methods, the training overhead needed, and the computational capacity available. In their approach, they leverage DL techniques to learn characteristics of past

channels and anticipate the optimal beamforming matrix for the future time instant to maximize the average achievable sum-rate of an ISAC system. By adopting this DL-based method, they eliminate the requirement for explicit channel tracking and achieve a significant reduction in signaling overhead. This means that it can effectively optimize the system's performance without the need for continuous channel tracking, leading to improved efficiency and resource utilization in ISAC systems. Additionally, by leveraging the penalty method, a versatile unsupervised DL based predictive beamforming design framework has been developed. This framework allows for the prediction of optimal beamforming configurations without the need for explicit supervision, enabling more efficient and adaptable beamforming techniques. The system model is summarized in Figure 3.

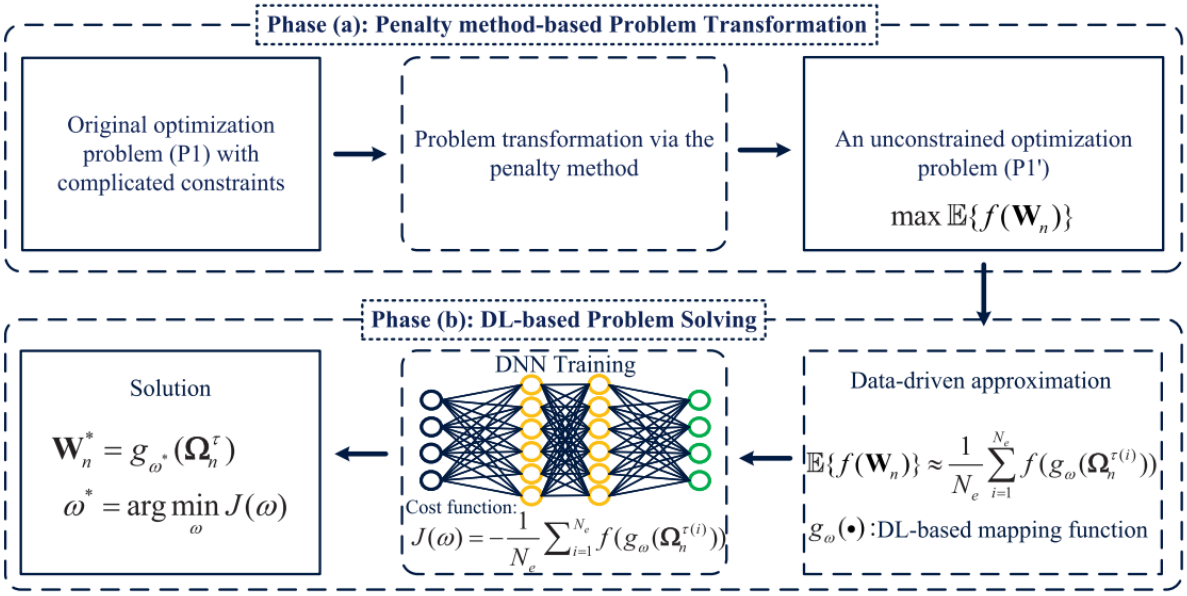

Figure 3. Predictive beamforming framework for ISAC [34].

2.4 Simulation frameworks for wireless communication

The digital representation of the real world is being extensively utilized in various applications, including 6G systems. This reduces the cost related to actual implementation of wireless systems and benefits from the rich contextual information to improve the performance of wireless systems and reduce the communication overhead. There are two main approaches where a simulation environment can become more beneficial,

1. *Generating datasets:*

   Learning-based methods like ML and DL are being investigated to optimize future communication networks' performance and capability. For example, physical layer optimization, network management and self-organization are some use cases where those data driven technologies come in useful. But these learning models need a large amount of data for the training process. It is not practical to build sensor aided wireless communication systems to test novel research ideas against improving the communication systems. Hence, specific simulation tools for future networks must possess the capability to handle not only

communication channels but also the corresponding sensor data that is relevant to the specific environment. This requirement ensures that the simulation accurately captures the interplay between communication and sensing aspects, enabling comprehensive evaluation and optimization of future network designs. Relatively, the research performed on 5G and 6G must deal with limited amount of data compared to other data driven applications such as large language models (LLM), etc.

These datasets will provide researchers with the opportunity to, develop deep-learning and computer vision algorithms specifically designed for sensor-aided wireless communication, evaluate the performance of these algorithms and compare them to existing approaches, reproduce and validate the results presented in other research papers in the field, establish benchmarks for various wireless communication problems, enabling fair comparisons between different proposed solutions using standardized data. According to the following table, there are already developed wireless data sets for different environments with various frequencies. And those datasets are actively used by the research community. By leveraging these datasets, researchers can advance the development in wireless communication and foster collaboration within the scientific community.

Table 3: Publicly available ray tracing datasets from simulation frameworks.

Dataset name	**Data types**	**Environment**	**Frequency (GHz)**
DeepMIMO [35]	Wireless channel	Both indoor and outdoor	2.5, 3.5, 28, 60
ViWi [9]	Image, point cloud, wireless channel and user location	Outdoor only	28, 60
Map based channel model [36]	Wireless channel	Both indoor and outdoor	28

2. *System testing:*

With 6G moving towards even higher frequency ranges like Terahertz frequency bands, it becomes even more challenging to do measurements or testing for this frequency range, specifically for outdoor scenarios. Considering that channel measurements for 6G will demand relatively expensive equipment, the simulation strategies for modeling the communication networks become more cost effective. Many devices utilizing large-antenna arrays are expected to incorporate additional sensors, including RGB cameras, depth cameras, or LiDAR sensors. This holds true for various applications such as vehicles, 5G phones, augmented reality/virtual reality (AR/VR) systems, intersection nodes for autonomous vehicles, and potentially even future base stations. These complementary sensors work alongside the large-antenna arrays to enhance the overall sensing capabilities and enable a more comprehensive understanding of the surrounding environment. The combination of these different sensors facilitates advanced functionalities and enables a wide range of applications in various domains. Adding those sensors will also become an extra cost for system testing.

Ailton Oliveira et al. proposed a machine learning based simulation platform [12]. The developed model is known as *Communication networks and Artificial intelligence immersed in virtual or Augmented Reality* (CAVIAR). The virtual world's 3D scenery can be created in two

ways: either from scratch by 3D design modelers or by importing data from the real world. In the first approach, 3D designs modelers create the virtual environment entirely using their skills and tools. In the second approach, data captured from the real world, such as satellite imagery, LiDAR scans, or photogrammetry, is imported and processed to generate the 3D representation of the real-world location in the virtual environment. It will be benefited to get more accurate communication results since it has real world data. This simulation model creates multi-model data for each discrete time $t \in \mathbb{Z}$, and can work in two types, the first type focus on online learning where it runs the simulation and the machine learning engine, creating a surrounding and data is transmitted in real time, or in discrete samples with time stamps given by the user. The second type of operation of the virtual simulation performs as a data recording to a database and use those recorded data later in for simulations and training neural networks. These two sub operations are called *INLOOP* and *OUTLOOP* methods respectively in the paper [12]. Therefore, for example, the system can handle simulations such as drone's trajectory deciding with reinforcement learning in real time and simulation of beam selection with the recorded data in non-real time.

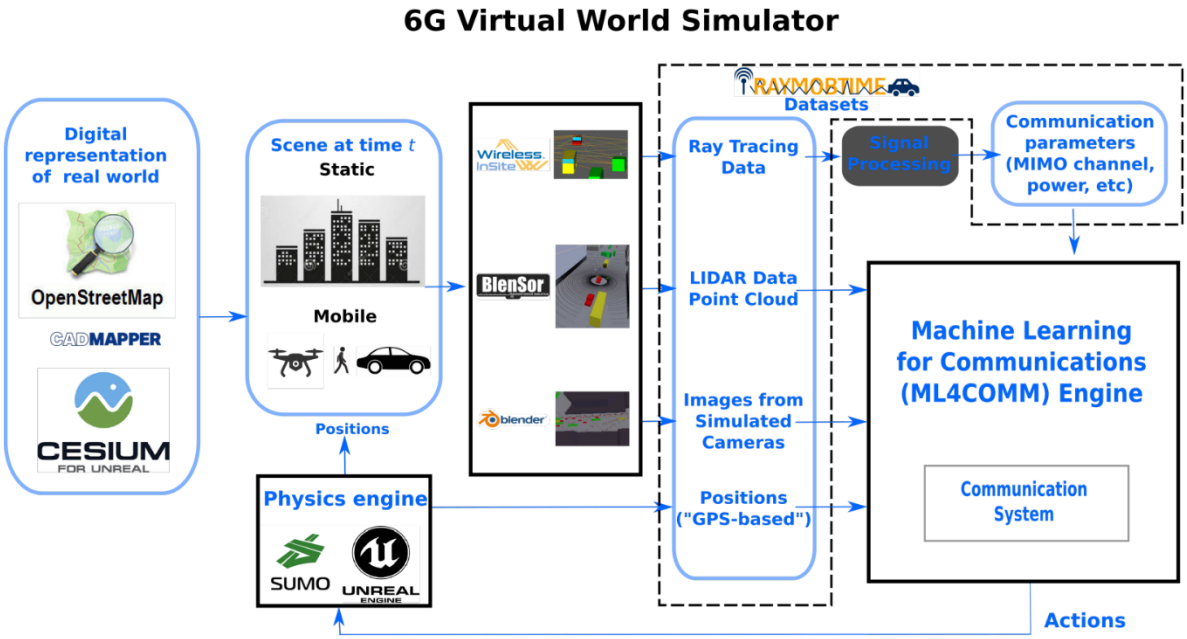

Figure 4. Block diagram of the CAVIAR simulation model [12].

Another example approach of using simulation frameworks, given by Afonso Oliveira et al. [13] The paper introduces a synthetic dataset generator for wireless mobile networks that incorporates a realistic mobility generation model and a diversified traffic generation model as in Figure 5. Generator can produce mainly three types of traces:

- **SNR traces:** Provide the position and SNR details at each instant of time with one trace per UE.
- **Traffic traces:** Provide the amount of information that is sent at each time instant with one per UE.
- **Aggregated trace:** For a specific time-window which has a pre given size, it provides the combination of traffic and SNR traces.

To generate the pedestrians and vehicles they used the SUMO emulator and to get a more realistic view of the environment OSM map is used, such that it can deliver the above-

mentioned traces more accurately. The process first processes information from the OSM map to create a static SNR map. Using this map, the Node processing module creates UEs based on the nodes obtained from the SUMO simulation and calculates the SNR traces for each UE. Subsequently, traffic traces are created by the Network traffic module. Lastly, the Dataset aggregation module combines the SNR and traffic traces into a single combined trace, allowing for comprehensive analysis and evaluation as in Figure 5.

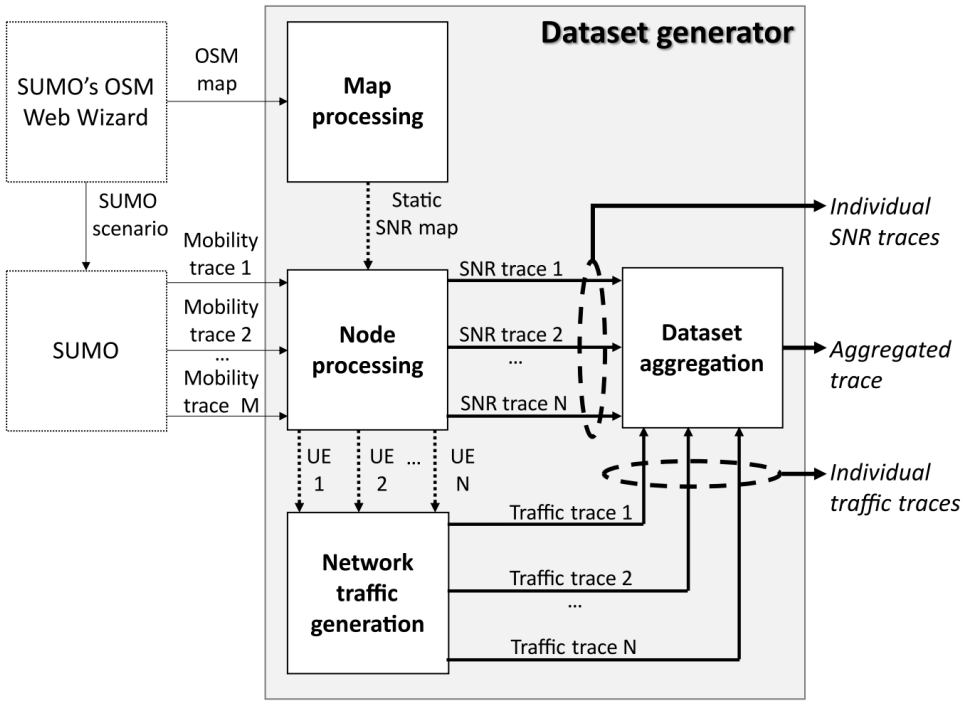

Figure 5. SNR and traffic synthetic trace data generator [13].

Most of the current research focuses on how data from actual sensors like LiDAR and cameras can be able to enhance communication performance using AI [10]. But the research related to such areas is limited due to the excessive cost, lack of mobility and control of the sensor equipped environment, lack of available data and it's with the hard applicability of sensor assisted systems. As shown in above literature, having 3D realistic models, physics engines and other virtual reality assets for simulations of communication systems, creates new areas and developments in terms of AI/ML applied to 6G and beyond.

2.5 Vehicle detection

Vehicle detection using point cloud data from LiDAR has garnered significant attention in recent years due to its potential applications in autonomous driving, traffic surveillance, and intelligent transportation systems. Numerous studies have explored various approaches and algorithms to tackle this challenging task.

There are mainly three approaches in detecting and tracking vehicles,

1. *Geometric feature based:*

These approaches utilize geometric properties of vehicles, such as shape and size, to detect them in point cloud data. Techniques like region growing, clustering algorithms (e.g., Density-based Spatial Clustering of Applications with Noise (DBSCAN)), or geometric primitives fitting (e.g., Random Sample Consensus (RANSAC)) are employed to segment point clouds into individual objects and identify vehicles based on their distinct geometric characteristics. The authors [37] solved this detection problem in three parts: point cloud clustering, bounding box fitting and point cloud recognition. The improved DBSCAN algorithm is used to cluster the point clouds and avoid the degradation caused by uneven distribution of LiDAR point clouds and the difference in clustering radius between point cloud clusters. The main idea of geometrical based vehicle detection includes mainly two steps. In the first step, the foreground and background components are separated from the captured data. This process enables the identification and isolation of the moving objects within the scene. The second step involves clustering the moving points into distinct categories, namely vehicles and non-vehicles. One such example is [38], where it uses raw point clouds to first identify interested regions, then do the ground removal, after that clustering and bounding box detection.

2. *ML and DL based:*

Using learning-based models has become the most preferred way of handling these substantial amounts of data. These approaches involve feature extraction from point cloud data and training a classifier on annotated data. Features can include local surface normals, histograms of oriented gradients (HOG), or more complex representations derived from the point cloud data. Commonly used classifiers include support vector machines (SVM), random forests, or neural networks Convolutional neural networks (CNNs), such as PointNet and its variants, are used to directly learn features from point clouds and classify them into vehicle and non-vehicle categories. These methods leverage the ability of deep networks to capture complex patterns and hierarchical representations from the point cloud data.

One 3D object detection type is to encode 3D LiDAR data into voxel grid, and then perform object detection based on the voxel grid features. VoxelNet paper [39] provides novel end to end deep learning architecture for point cloud-based 3D detection. By working directly with the sparse 3D point data, VoxelNet aims to streamline the process and improve the efficiency and accuracy of object detection and recognition tasks. By avoiding the manual feature engineering step, VoxelNet offers a more streamlined and effective approach for processing sparse 3D point data.

Anusha et. al [40] use a recurrent based learning method to detect vehicles using LiDAR data. Instead of analyzing the entire point cloud, the network acquires the ability to identify specific areas of interest, allowing for a substantial reduction in the number of points that need to be processed and the time required for inference. This is a novel end-to-end trainable deep architecture for object detection in point clouds.

3. *Sensor fusion method:*

Sensor fusion involves combining point cloud data from LiDAR sensors with data from other sensors, such as cameras or radar. By fusing data from multiple sensors, complementary information can be utilized to improve the accuracy and robustness of

vehicle detection. Fusion approaches can employ techniques like data fusion at the feature level, decision level fusion, or even fusion at the deep network level.

The proposed method in [41] incorporates radar, LiDAR and camera sensors. This fusion approach extracts the advantages of multiple sensors, for example, LiDAR data can give a good estimation of the distance to the object and its size while camera can classify the object accordingly. This proposed solution addresses the challenge of detecting and tracking moving objects by introducing a comprehensive perception fusion architecture. This architecture is built upon the evidential framework and incorporates composite representation and uncertainty management techniques.

Xiangmo et. al [42] provided with a fusion vehicle detection method using LiDAR and camera. First, they used the point cloud data to create accurate object-region proposals, then these are mapped into the image space which used to get the Region of Interest (ROI). The selected region is then fed into CNN for object recognition. Also, they achieved real-time detection with only 66.79 milliseconds average processing time.

3 SIMULATION PIPELINE

The implementation of a dynamic simulation environment to create data sets for a system with LiDAR cohabiting with a 5G New Radio (NR) compliant wireless system is presented. The base of the vehicular traffic scenario is defined according to the 3rd Generation Partnership Project (3GPP) compliant documents. LiDAR performance in an outdoor traffic scenario was tested with a vehicle detection and localization algorithm. As an important part of the study, the behavior of LiDAR in urban vehicular traffic scenarios is observed under different changing parameters like LiDAR scan radius, scan resolution, and height from the ground. In addition, a vehicle localization algorithm is used with obtained point cloud data from the LiDAR to measure how well the vehicle detection can be done and what kind of accuracy can be achieved for different variable parameters. This study of performance evaluation of detection accuracy is done using a custom-developed error model. After that, a novel method of performing beamforming with less wireless overhead is given.

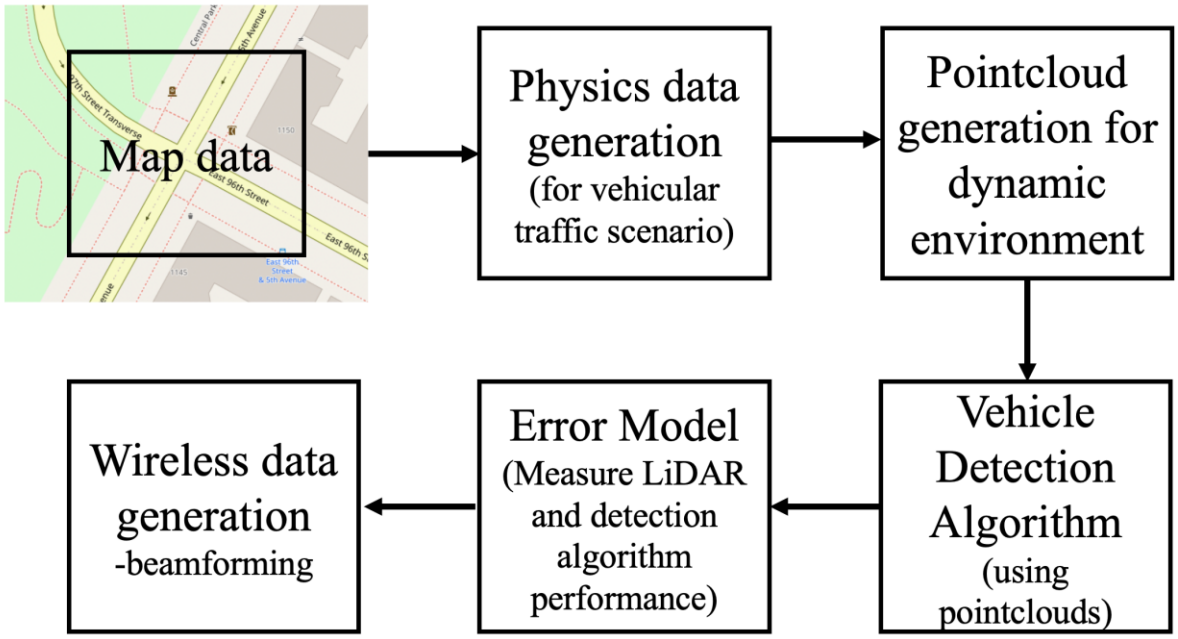

Figure 6: Simulation pipeline overview.

3.1 Environment selection

According to 3GPP compliant document ETSI TR 138 913 section 6.1.4, [43], the selected environment is called, "Urban Macro". The key characteristics of this scenario are continuous and ubiquitous coverage in urban areas. This scenario will be interference-limited, using macro TRxPs (i.e., radio access points above the rooftop level). In this simulation environment, the focus will be UE inside moving vehicles.

Therefore, in a vehicular traffic scenario, multiple junctions from Manhattan in the United States are selected as the simulation environment (Figure 7). The reason for selecting the Manhattan area is to have generalized junction traffic with multiple lanes. Some main roads of the area include up to four lanes, which helps to test the detection capability and LiDAR performance in all types of traffic (low, moderate, and high) without changing the environment.

These different traffic types are achieved by changing the vehicle insertion density parameter of the physics engine. "OpenStreetMap" [44] is used to collect map data of a particular junction. These map data were used for the physics engine later.

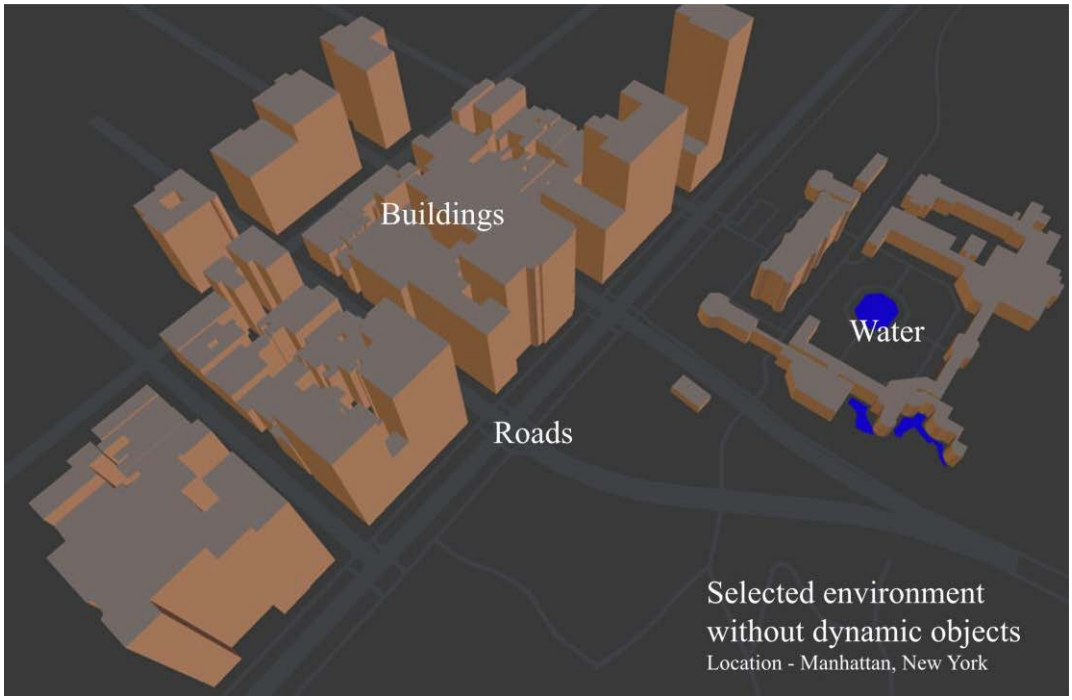

Figure 7: Example vehicular road environment without dynamic objects.

3.2 Physics engine

To achieve dynamic changes, vehicles should have motion according to general traffic rules. Therefore, the generation of vehicle paths and velocities has been achieved with the "Simulation of Urban Mobility" (SUMO) [45] open-source package. This is a microscopic, multi-model traffic simulator. It allows doing a simulation of how a single vehicle moves through a road with given traffic demand and a given road network.

Vehicles are modeled explicitly, have their own route, and do not depend on other vehicle routes. Even though the simulations are deterministic by nature; there are diverse options to introduce randomness in multiple levels using this simulator. For this study, randomness is used to check the pipeline's robustness. Randomness can be changed using a seed value. The road network can be changed according to requirements. For example, there can be multiple edges between two junctions as there can be multiple lanes on the road. Network files can be edited using the Netedit GUI tool provided by SUMO to get the required junctions and edges. Routes are created by randomly selecting source and destination edges according to a Poisson distribution. Physics engine workflow shown in Figure 8.

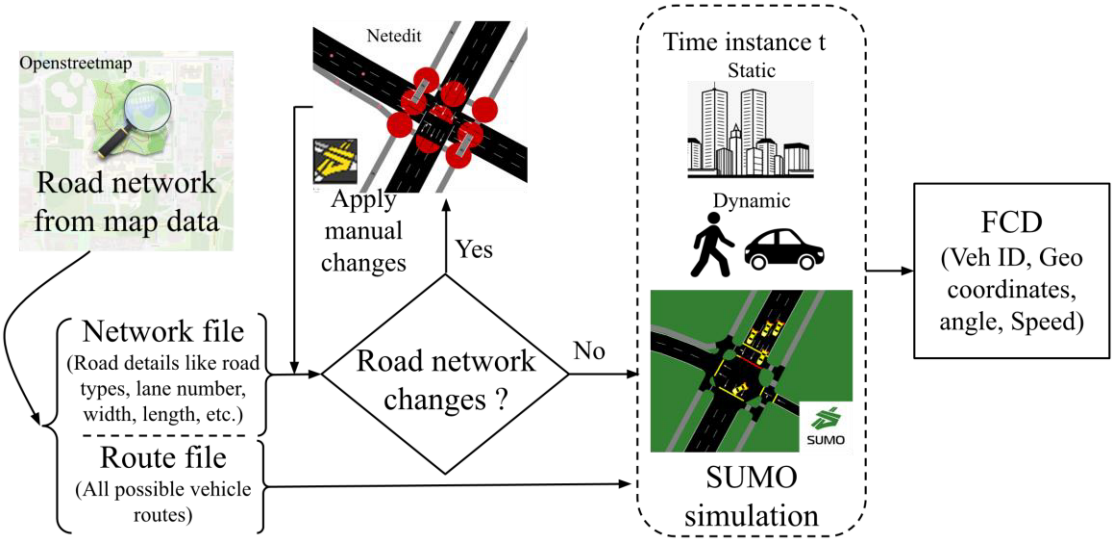

Figure 8: Physics engine to generate vehicular motion data.

Table 4: Physics data generation parameters.

Parameter	**Value**	**Explanation**
Run time	1200 seconds	Ensure enough vehicle movements are captured from the LiDAR.
Vehicle insertion rate	1 vehicle per second	Provide the traffic density which is closer to natural urban city environment.
Minimum distance	300 m	Ensure that every vehicle will travel at least minimum distance which reduces the random vehicle spawning in the middle of the road.
Maximum vehicle speed	30 Kmph	According to ETSI TR 138 913 section 6.1.4 [43] for high urban city area the maximum vehicle speed is selected
Fringe factor	10	Ensures that vehicles start and end their trips at the edge of the road network. Then LiDAR sensor should not capture missing and teleportation of vehicles on the road

Table 4 presents some crucial parameters used for physics data generation. As for the data output SUMO provides a configuration file type called Floating Car Data (FCD), which includes vehicle position, vehicle speed, lane id and vehicle angle with timestamps.

3.3 LiDAR point cloud generation in dynamic environment

To facilitate the sensing aided communication, the main sensor was selected as the LiDAR. Selected LiDAR is Velodyne HDL-64E2. But this is a simulation environment, sensor parameters can be changed according to the user requirements. This laser scanner was added using the open-source project Blensor [46] in Blender software.

Table 5: LiDAR configuration.

LiDAR model	Velodyne HDL-64E2
Scan resolution	0.1m
Rotation speed	30 Hz
Scan distance	100 m
Added noise distribution	Gaussian
Mean of added noise	0 m
Standard deviation of added noise	0.01 m
Decibel noise standard deviation	0.08 dB
Start angle	0 degrees
End angle	360 degrees
Reflectivity distance	50 m
Reflectivity limit	0.1 m
Reflectivity slope	0.01 m

Dynamic simulation of the environment in Blensor is achieved using a blender python [47] Application Programming Interface (API). This will extract the information from physics data file and place car objects in particular locations throughout the timeline. These individual timestamps are called "key frames" in the Blender software. After generating keyframes, the simulation can run where cars move in the 3D environment according to previously generated physics data. Then point cloud data can be extracted for each frame. The transition of developing the dynamic environment from the physics data is achieved using a blender python API. The process of the transition is shown in Figure 9.

Figure 10 illustrates an example environment created in Blender, along with the corresponding acquired point cloud data. Vehicles are visible in the point cloud data with Table 5: LiDAR configuration. Minor changes of the scan resolution parameter significantly change the size of point cloud data. According to Figure 10 right hand side point cloud visualization, the density of the points reduces with the scan distance. Vehicle may not capture from the LiDAR due to the high gap between LiDAR point cloud rings which are far more away from the sensor. Therefore, getting more than 100 m scan distance will reduce the vehicle detection accuracy and that added data points won't be any useful. Furthermore, LiDAR height effects the blind spot radius. When increasing the LiDAR height, even though you get a higher point cloud density at far areas from the LiDAR; larger blind spot will affect the near areas significantly. These phenomena are thoroughly studied in the latter sections using the custom error model.

Users can also increase the noise level added from the LiDAR to get more practical datasets, which is more like to actual traffic junction environment.

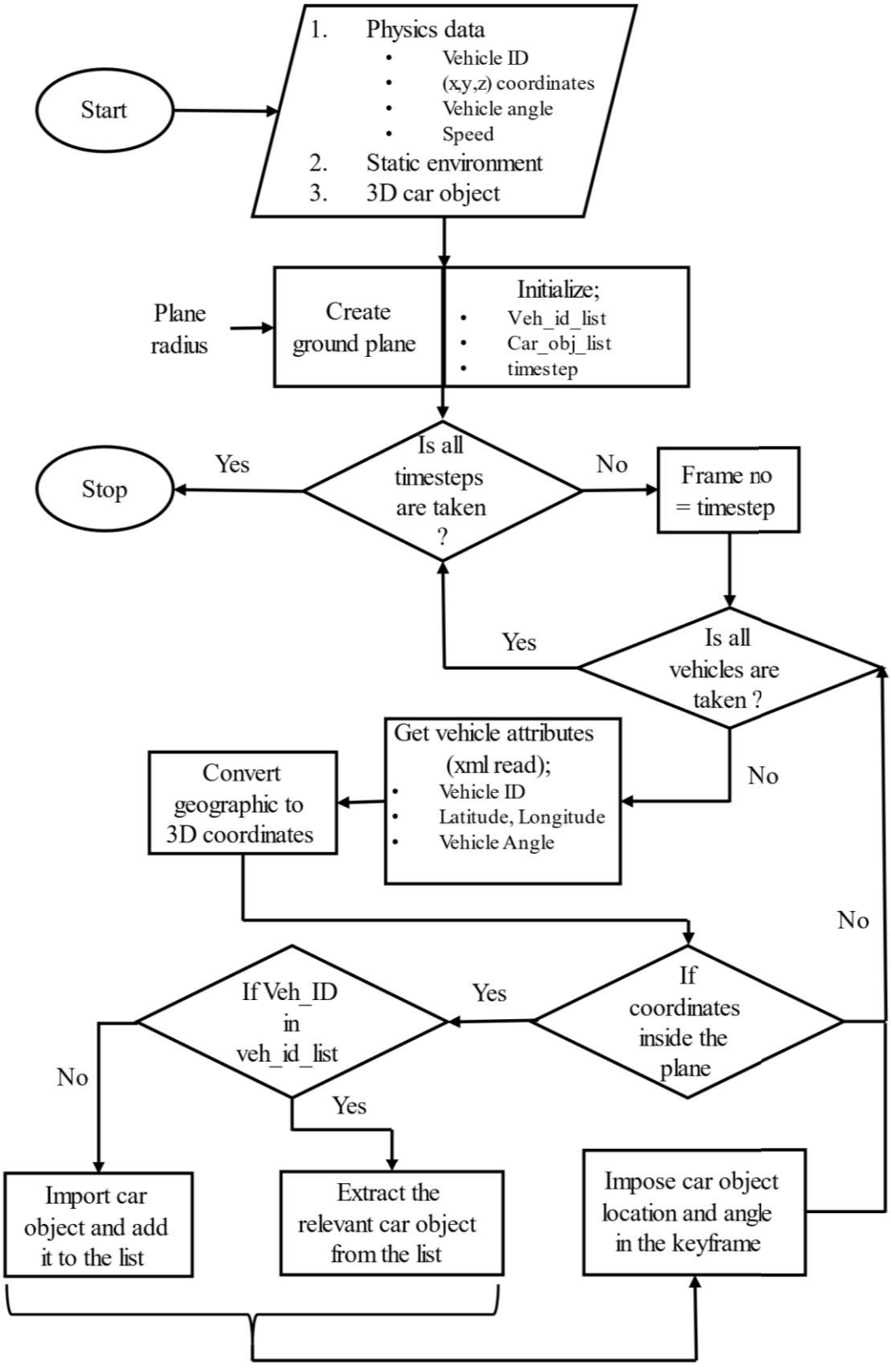

Figure 9: Transition algorithm to create dynamic environment from physics data.

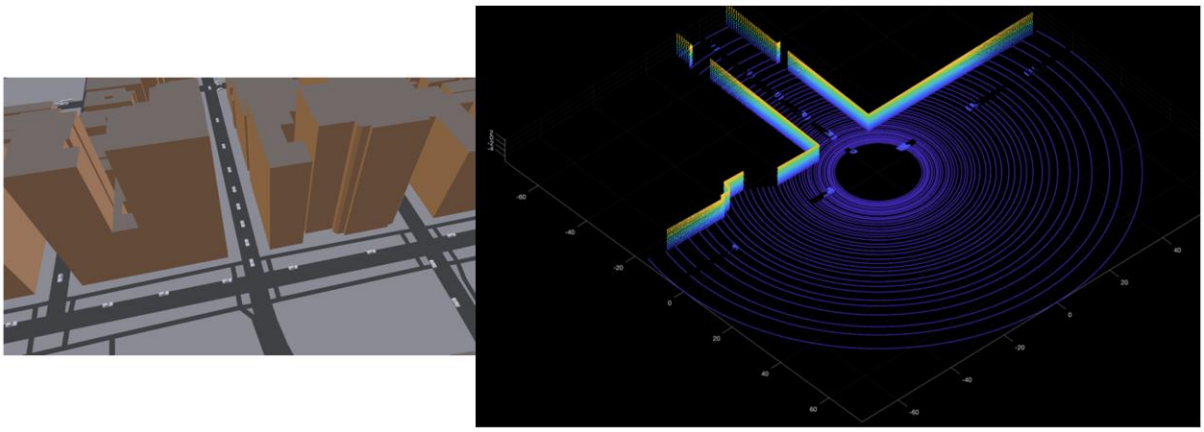

Figure 10: 3D environment (left) and its corresponding point cloud (right). LiDAR is in the middle of junction.

3.4 Vehicle detection

Sensing aided wireless communication research requires datasets with ability to simulate and acquire information from sensing agent. In this study, the simulation pipeline for an urban scenario to reduce the wireless overhead with LiDAR requires an algorithm which can detect vehicle locations from point cloud data. Several types of methods such as machine learning and ground plane removal with cluster-based can be used to get vehicle locations.

Since point cloud data generated from a simulation platform, using a learning algorithm like in [39] has a high probability to overfit the model to the data. Even if we make the simulation to more practical environments, there is an excessive cost of training since the input data type (point cloud) consists of large size data files. Also, most of the learning algorithms require LiDAR intensity data which is not available from Blensor API. Therefore, ground plane removal with cluster-based method [38] is identified as more suitable for the simulation pipeline.

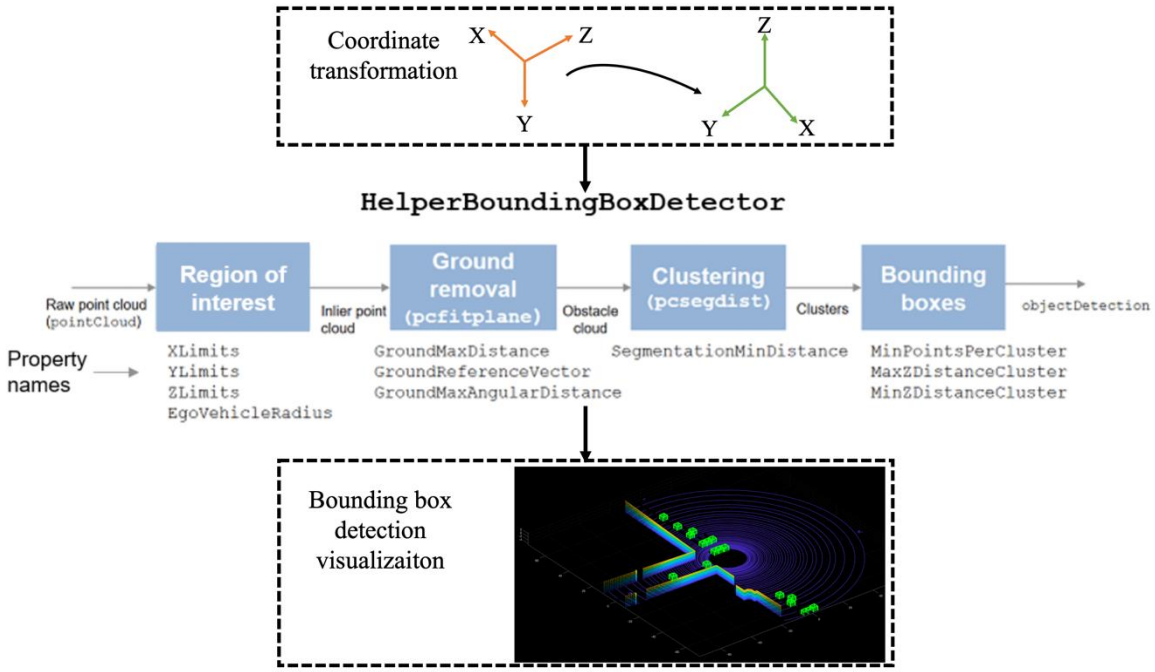

Figure 11: Vehicle detection algorithm.

Before feeding point cloud data into the clustering algorithm, it needs to go through a data preprocessing step where change of axis needs to happen (Figure 11). Because point cloud data taken from LiDAR needs to transform into the global coordinate system (Figure 12).

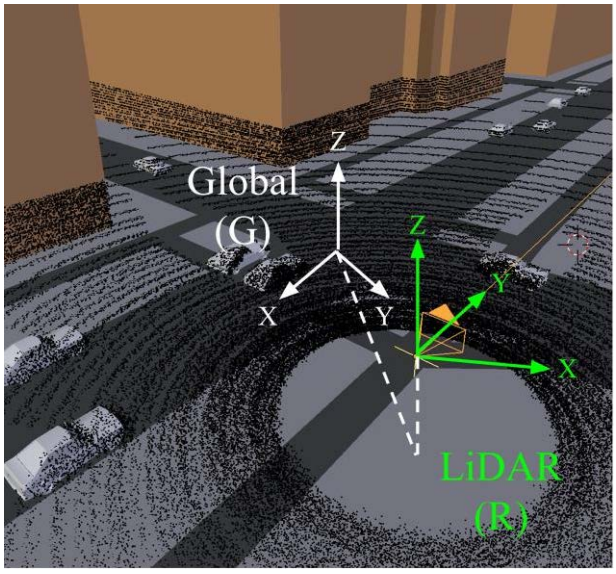

Figure 12: Global and LiDAR coordinate systems visualization.

Homogenous transformation matrix H which transforms roadside LiDAR unit point cloud data to global coordinates can be divided into rotation R matrix and translation t matrix from global to LiDAR,

$$R = \begin{bmatrix} \cos\theta\cos\psi & \sin\phi\sin\theta\cos\psi - \cos\phi\sin\psi & \cos\phi\sin\theta\cos\psi + \sin\theta\sin\psi \\ \cos\theta\sin\psi & \sin\phi\sin\theta\sin\psi + \cos\phi\cos\psi & \cos\phi\sin\theta\sin\psi - \sin\phi\cos\psi \\ -\sin\theta & \sin\phi\cos\theta & \cos\phi\cos\theta \end{bmatrix} \tag{3.1}$$

where ϕ, θ and ψ specify the intrinsic rotation angles around the x, y and z axis of global coordinate system, respectively. t be shown as,

$$t = \begin{bmatrix} t_x \\ t_y \\ t_z \end{bmatrix} \tag{3.2}$$

Then the corresponding H can be written as,

$$H = \begin{bmatrix} R_{3\times3} & t_{3\times1} \\ 0_{1\times3} & 1 \end{bmatrix} \tag{3.3}$$

Finally, corresponding global point with respect to LiDAR point can be derived as,

$$P_{global} = H \cdot P_{LiDAR} \tag{3.4}$$

Where both P_{global} and P_{LiDAR} will have 4×1 dimension and first 3 values represent the 3D coordinates. After getting 3D coordinates relative to the global coordinates pipeline, the main vehicle detection algorithm runs.

The main algorithm consists of four parts which are explained as below,

1. Region of Interest

Parameters – X, Y, Z limits of the environment and blind spot radius.

Point cloud data might have unwanted regions where you do not have to process to get vehicle detections. Therefore, as for the first step, algorithm limits the point cloud processing region according to user range input from distances along x, y and z axis. To further increase the processing speed, it is possible to provide the ego vehicle radius such that the algorithm won't consider that circular region as well. But in this case, the LiDAR is mounted at roadside and the blind spot created by the LiDAR will not provide any point cloud information, hence it is not necessary provide a value to the parameter 'EgoVehicleRadius'.

2. Ground Removal

Parameters – Maximum distance that ground plane points can exist, ground reference vector, maximum angular distance of point to reference vector.

In ground scenes, ground points occupy a sizable portion of the point cloud data, and the objective is to remove the static environment and focus on the dynamic objects, here its vehicles. 'pcfitplane' MATLAB function is used to remove the ground plane. The added Gaussian noise for the simulated LiDAR point cloud directly affects the maximum distance that points of the ground plane can exist. Therefore, the value for that parameter is selected manually and it should be only the maximum distance through the ground plane reference vector between any two ground points. Since ground planes can have angles to the global coordinates, the perpendicular reference vector to the ground plane must be provided. The algorithm also takes the maximum angular distance a ground plane point can take from the reference vector to determine the boundaries of the ground plane.

3. Clustering

Parameter – Minimum segmentation distance between two clusters

After the ground points are removed, the point clouds in the environment become independent clusters. MATLAB 'psegdist' function used for the Euclidean distance-based clustering [48] method to cluster the points with close distance into one class and only the coordinate information of the points is used in the clustering. Since this is a simple simulation environment and objective is to find out the LiDAR performance and wireless signal behavior in dynamic situation, there are no other objects except vehicles. Therefore, Euclidean based clustering can be applied to this scenario. But if there are other objects like bushes then to identify those objects separately, we need the intensity information of the LiDAR. Vehicles and bushes have different reflection intensity due to the significant difference in material. In a practical environment with an actual LiDAR the identification of various objects is also possible.

4. Bounding boxes

Parameters – Minimum number of points per cluster, maximum and minimum z coordinate for cluster

Each detected cluster from the clustering part is converted to a bounding box detection with the format $[x, y, z, \theta, l, w, h]$. Where x, y, z refers to the point position of the bounding box, θ refers to the yaw angle and l, w, h refers to its length, width, and height. Parameter with minimum number of points per cluster make sure that small clusters due to the point cloud noise will not detect as vehicles. High number of this parameter will result in not detecting the cars that far away from the LiDAR sensor, which contains a smaller number of points in the cluster, but at the same time less number for this parameter will increase the false positive detections where the algorithm detects multiple clusters even though there is only one vehicle in the actual scenario. Therefore, to achieve better accuracy for the detection algorithm, one can use a grid search to identify the optimum value for that environment. Maximum and minimum distance through z axis represents the vehicle height in coordinate system values.

After the bounding box detection, those boxes are visualized against the point cloud obtained from the simulated LiDAR to check the algorithm performance and this visualization is used for the fine tuning of some parameters in the detection algorithm.

3.5 Error model

The custom error modelling algorithm is developed to identify the performance of any given vehicle detection algorithm using point cloud data and LiDAR performance with different parameters. This custom model can be used for vehicular traffic scenario environment after initial input parameter modifications. The calculated results from the algorithm are detection accuracy, false negative and false positive detections. The algorithm contains a visualization part where it shows multiple useful information related to detection and LiDAR capability.

For the calculation of error introduced by the detection algorithm and LiDAR, it is necessary to have actual correct locations to compare with the detection algorithm output locations of vehicles. Since this is a simulation environment it is possible to extract actual location data from the SUMO physics engine. A python script is used to read the vehicle locations from the physics engine, FCD data output. Script access the FCD xml file and read to extract X, Y and Z coordinates of generated vehicle positions from the physics engine. These data are converted to floating point number types from string type while extracting and written into a csv (comma separated values) file. Additionally, running of the detection algorithm is done separately and those detected vehicle locations are also written into a csv file. These detection and actual positioning data will be accessed later from the error model.

Table 6: Extracted data from physics engine and bounding box detection algorithm.

Time instance	**Physics engine data**		**Bounding box detection**
	Vehicle ID	**Location**	
t_i	I_m	$S_{m,i} = (x_{m,i}, y_{m,i}, z_{m,i})$	$BB_{i,1} = (x_{i,1}, y_{i,1}, z_{i,1})$
	I_n	$S_{n,i} = (x_{n,i}, y_{n,i}, z_{n,i})$	$BB_{i,2} = (x_{i,2}, y_{i,2}, z_{i,2})$
	.	.	.
	.	.	.

$i \in \mathbb{Z}^+$	$m, n \in \mathbb{Z}^+, m \neq n$ There can be multiple IDs under one t_i. These vehicle IDs have the possibility to appear in another t_i.	Bounding box locations do not have vehicle ID since it's detected from the LiDAR data.
The number of data points in physics and bounding box detection might not be the same number for a single time instance.		

The Z coordinate from physics data is not required since all vehicles have the same Z coordinate (height of the vehicle) for this simulation scenario with flat ground. But Z coordinate is necessary for simulation of vehicular traffic environment with diverse terrains and the code can be modified easily to achieve that. Also, the Z coordinate identified from the vehicle detection algorithm carries a meaning to identify false negative and false positive detections, which will be discussed in the results section of the error model.

Algorithm takes several inputs like LiDAR height, car height, LiDAR location, transformation matrix, error threshold, boundary area and file locations which contains bounding box detection and physics simulation positions. First, it finds out the intersection timestamps between detection and physics data. Then loop through each common timestamp and process each frame using following five parts,

1. *Nearest point matching:*

   One point cloud frame can contain multiple vehicles. Therefore, one timestamp will have multiple data entries from both vehicle detection algorithm and physics simulation. The objective is to map each bounding box vehicle location from detection algorithm into actual location from physics data.

   To achieve this objective, after the homogenous transformation of LiDAR coordinates the algorithm creates two arrays with bounding box and physics data locations, then those arrays are used to identify the nearest LiDAR coordinate to the actual point using 'dsearchn' inbuilt MATLAB function. This will provide LiDAR array index to the actual nearest location and the Euclidean distance between two closest points in 3D space.

2. *False positive (FP) detection:*

   Provides vehicles that falsely detected from the vehicle detection algorithm when there is no actual vehicle from physics engine.

   With the derived pointing index algorithm, potential false positive detections can be found while going through the matched arrays in the above part. This potential FPs are taken if there are more than one bounding box locations points to same actual location. If the potential FP array is not empty, then algorithm goes to a different branch using if condition to get the corresponding bounding box location that is nearest to the actual location from physics engine. This selection is done from previously acquired FPs related to one actual location. Finally get the result bounding box coordinates which do not correspond to FPs.

3. False Negative (FN) detection:

   Provides not detected vehicles from detection algorithms when there are actually vehicles from the physics engine.

   Use of detected FPs from above step in the algorithm is adopted to this section to identify FNs. If the number of physics engine locations are greater than bounding box locations after removing FP detections, then remaining additional physics engine locations will be flagged as FNs.

4. Correct (True Positive (TP)) detection:
   Provides correctly detected vehicles with minimum Euclidean error distance between detected and actual vehicle location.
   TPs are then equal to the bounding box locations after removed FPs.

5. Visualization:
   Error models provide mainly three visualizations.
   - 2D map where FPs, FNs, TPs and physics engine vehicle locations (Figure 19) for a time instance
   - histogram of bounding box Euclidean distance error (Figure 20) for a time instance.
   - The variation of Euclidean distance error with the LiDAR point distance. Also, this graph includes FP and FN counts with the LIDAR point distance. (Figure 21)

Pseudo code of the error modelling algorithm,

Algorithm 1: Error Model

Inputs: Bounding box locations:(L_{bb}) and simulated vehicle locations:(L_s) with timestamps. LiDAR radius:(r). LiDAR sensor position coordinates:(X). Transformation matrix from LiDAR to global coordinates (H)
Update: L_s with coordinates only inside the LiDAR scan radius
Update: $L_{bb}$with transformed coordinates using H
Get intersection timestamps $T = (t_1, t_2, \ldots\ldots, t_n)$ of L_{bb} and L_s
for t in T **do**
    Returns the indices of the closest points in $L_s(t_i)$ to the query points in $L_{bb}(t_i)$ ▷ **Comment 1**
    $L_{potential\_FP}(t_i)$ = Identify $L_{bb}(t_i)$ coordinates that points to a same location in $L_s(t_i)$
    if $L_{potential\_FP}(t_i)$ is **NOT** empty **then**
        $L_{bb\_NOT\_FP}(t_i)$= Get the coordinate from $L_{potential\_FP}(t_i)$ which has minimum distance to corresponding coordinate in $L_s(t_i)$
        $L_{FP}(t_i)$ = Remove $L_{bb\_NOT\_FP}(t_i)$ from $L_{potential\_FP}(t_i)$)
    else
        $L_{FP}(t_i)$ = **Nan**
    end if
    if length($L_s(t_i)$) > **length**($L_{bb\_NOT\_FP}(t_i)$) **then**
        $L_{FN}(t_i)$ = Coordinates in $L_s(t_i)$ except $L_{bb\_NOT\_FP}(t_i)$
    else
        $L_{FN}(t_i)$ = **Nan**
    end if
    $L_{TP}(t_i) = L_{bb\_NOT\_FP}(t_i)$
end for
Outputs: $L_{TP}(t_i)$ $L_{FP}(t_i)$), $L_{FN}(t_i)$ ▷ **Comment 2**

Comment 1: There can be more than one instance where queried bounding box locations points to the same simulated vehicle location. Which gives potential FPs from the vehicle detection algorithm.

Comment 2: False positives are locations where the vehicle is not supposed to be. True positives (TP) are bounding box detection without false positives which means correct locations from the vehicle detection algorithm. FNs are locations where a vehicle detection algorithm does not detect a vehicle.

3.6 Precoder based wireless beamforming

Beamforming is a technology where the radiation pattern of MIMO antenna steers according to the UE direction to achieve high QoS in a wireless channel. Beam formed radiation pattern for a specific azimuth and elevation angle can be calculated according to [49]. There it gets the element pattern by separately calculating horizontal and vertical radiation pattern in decibel. Then composite array radiation is added to already calculated element pattern to get the beam formed radiation pattern for all elevation and azimuth angle range. The composite radiation pattern is calculated using weighting factor, steering matrix components and correlation level.

The theoretical background of MIMO beamforming is explained in section 2.3 under Intelligent beamforming. Here the explanation of practical implementation of precoder based beamforming is presented.

The objective is to get a composite array pattern for a uniform rectangular array (URA) MIMO antenna with precoder weights as in Figure 13. The effect of precoder weight is added to the element pattern of the antenna to get composite array pattern.

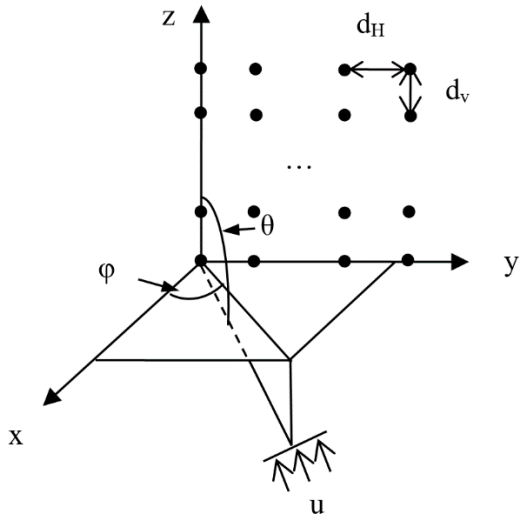

Figure 13: Geometric representation of MIMO URA antenna.

The considered URA antenna has $N_V \times N_H$ radiation elements for modelling. The numbers of the elements placed along y-axis and z-axis are N_H and N_V, respectively.

The array factor of the planar array can be represented by $\widehat{W}$, i.e.,

$$\widehat{W} = W \cdot V \tag{3.5}$$

where V represent the phase shift due to array placement, given as,

$$V = \left[v_{1,1}, v_{1,2}, \dots, v_{1,N_V}, \dots., v_{N_H,1}, v_{N_H,2}, \dots, v_{N_H,N_V}\right]^T \tag{3.6}$$

$$v_{m,n} = exp\left(i \cdot 2\pi\left((n-1)\cdot\frac{d_V}{\lambda}\cdot cos(\theta) + (m-1)\cdot\frac{d_H}{\lambda}\cdot sin(\theta)\cdot sin(\varphi)\right)\right) \tag{3.7}$$

$$m = 1,2,\dots N_H; n = 1,2,\dots N_V;$$

Then, W is the precoder weighting factor. This can provide control of side lobe levels and can also provide electrical steering, both horizontal and vertical. The assumption is, for all radiation elements weighting vector will be identical. Weight vector is given as,

$$W = \left[w_{1,1}, w_{1,2}, \dots, w_{1,N_V}, \dots., w_{N_H,1}, w_{N_H,2}, \dots, w_{N_H,N_V}\right]^T \tag{3.8}$$

$$w_{m,n} = \frac{1}{\sqrt{N_H N_V}} exp\left(i \cdot 2\pi\left((n-1)\cdot\frac{d_V}{\lambda}\cdot sin(\theta_{etilt}) - (m-1)\cdot\frac{d_H}{\lambda}\cdot cos(\theta_{etilt})\cdot sin(\varphi_{escan})\right)\right),$$

$$m = 1,2,\dots N_H; n = 1,2,\dots N_V; \tag{3.9}$$

where θ_{etilt} is electrical down tilt steering angle and φ_{escan} is electrical horizontal steering angle.

The phase of weighting vector is used for the electrical steering according to our requirement. Change of θ_{etilt} will steer the beam in zx plane (elevation plane) while φ_{escan} will steer the beam in xy plane (azimuth plane).

Then the composite array radiation pattern is given by $A_A(\theta,\phi)$ as,

$$A_A(\theta,\phi) = A_E(\theta,\phi) + 10\,log_{10}\left[1 + \rho\cdot\left(\left|\sum_{m=1}^{N_H}\cdot\sum_{n=1}^{N_V} w_{m,n}\cdot v_{m,n}\right|^2 - 1\right)\right] \tag{3.10}$$

The element pattern is given by $A_E(\theta,\phi)$,

$$A_E(\theta,\phi) = G_{E,max} - \min\{-[A_{E,H}(\phi) + A_{E,V}(\theta)\,], A_m\} \tag{3.11}$$

where,

$$A_{E,V}(\theta) = -min\left[12\left(\frac{\theta-90}{\theta_{3dB}}\right)^2, SLA_v\right] \tag{3.12}$$

$$A_{E,H}(\varphi) = -min\left[12\left(\frac{\varphi}{\varphi_{3dB}}\right)^2, A_m\right] \tag{3.13}$$

where $G_{E,max}$ is 8 dBi which corresponds to 18 dBi antenna array gain, SLA_v is side lobe lower level which is taken as 30 dB and A_m is front-to-back ratio which is taken as 30 dB.

Generated radiation pattern (Figure 14) from above equations is given in FigureFigure 14, for 8x8 MIIMO antenna as an example.

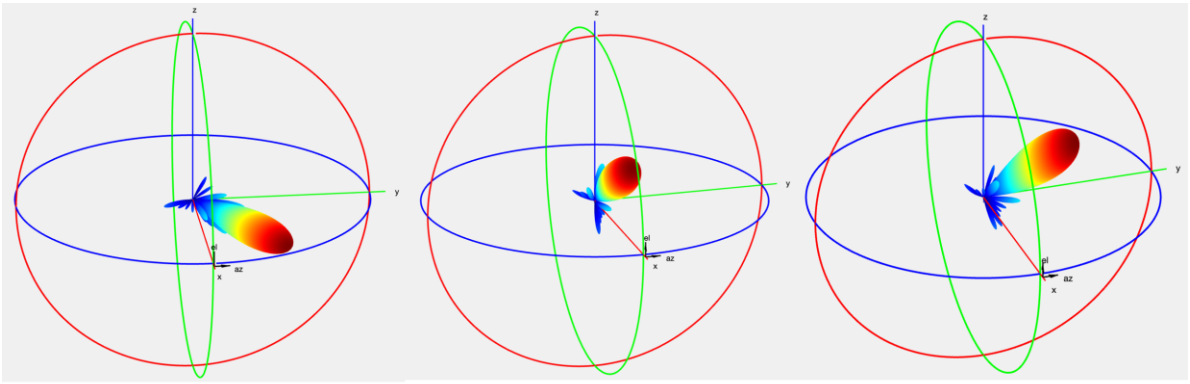

Figure 14: Beam formed radiation patterns in degrees for three instances of azimuth and elevation electrical steering angles for 8x8 MIMO antenna.

Precoder based beamforming is implemented as in MATLAB code to steer the radiation pattern on to specific part of the road, according to the simulated vehicle location from the pipeline. Detected vehicle location information is used and generated a novel periodic beam map to reduce the wireless communication overhead in vehicular traffic communication provided in the results section.

4 RESULTS AND DISCUSSION

The performance and observations from the proposed simulation pipeline with sensing assisted novel beamforming method were evaluated through a selected vehicular traffic scenario as in section 3.1 Environment selection.
Results from the study are three-fold,

- Resulting observations of having LiDAR as a RSU in vehicular traffic scenarios and LiDAR characteristic discussion with controllable parameters.
- LiDAR performance and its detection error variation using custom developed error model.
- Novel method of using periodic wireless beamforming road map to reduce overhead of V2I communication.

4.1 LiDAR characteristics against controllable parameters

Even though the main use of having LiDAR as a RSU in ISAC context is to improve communication, it is necessary to study the behavior of a LiDAR. One of the main parts of this study is to identify the characteristics of roadside LiDAR in an urban traffic environment. LiDAR performance change discussed in following sections with variable parameters such as LiDAR height, scan resolution, added artificial Gaussian noise and maximum scan radius.

- *LiDAR height*

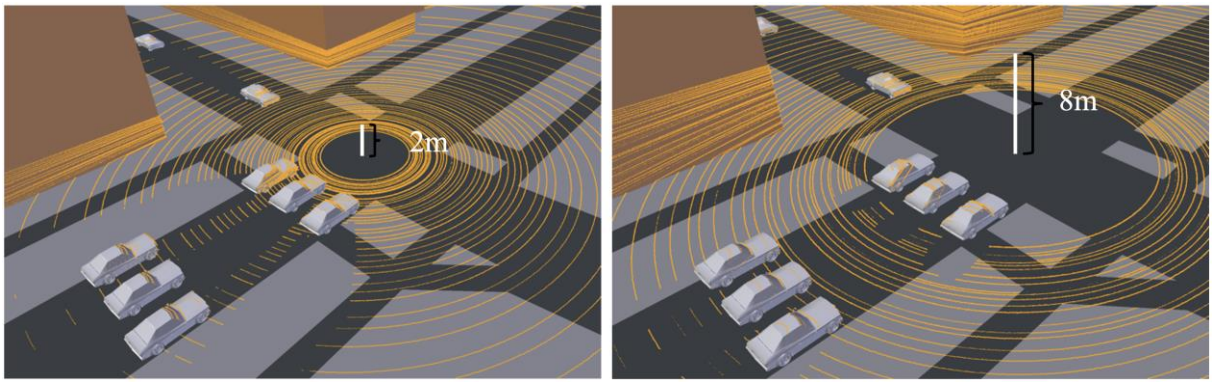

Figure 15: Point cloud visualization for 2m (left) and 8m (right) LiDAR heights.

When increasing the LiDAR system's height (Figure 15), the resulting blind spot radius also increases, which hinders detection of a significant number of vehicles when the LiDAR is mounted close to the road. Conversely, lower LiDAR heights lead to the occurrence of elongated shadows cast by objects, such as vehicles located near the sensor, resulting in multiple blind spots within the sensing region that extend beyond the primary blind spot circle. To mitigate these issues, it is possible to install the LiDAR system at a distance from the road, thereby avoiding the direct formation of the main blind spot circle and reducing the impact of shadowing caused by nearby objects. By strategically positioning the sensor, the blind spot circle can be circumvented without compromising detection capabilities. However, there are instances where it becomes necessary to mount the LiDAR on traffic poles to minimize additional infrastructure costs. Nonetheless, this arrangement introduces a primary blind spot

on the road due to the proximity of the traffic poles. Consequently, it is imperative to conduct a thorough investigation to determine the optimal LiDAR height that minimizes both the blind spot radius and the shadowed area. Furthermore, by analyzing past vehicle locations, it is possible to predict vehicle trajectories within the blind spot and shadowed areas. This approach can alleviate the challenges associated with acquiring accurate vehicle locations in regions where laser points are absent.

- *Scan resolution (laser point density)*

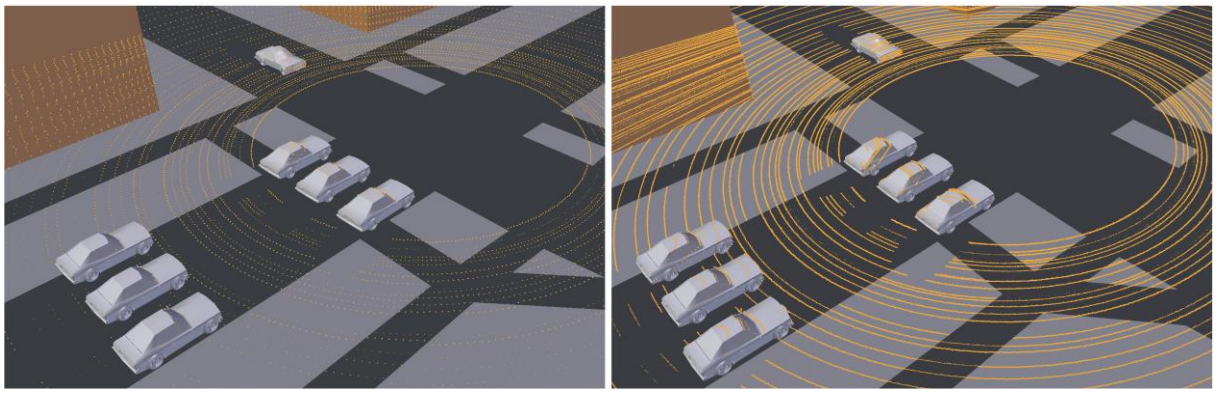

Figure 16: Point cloud visualization for low (left) vs high (right) point cloud densities.

In a simulation environment, the scan resolution can be adjusted at will; (Figure 16) however, in real-world applications, the scan resolution is dictated by the specifications of the sensor being used. A higher point density can result in improved accuracy of car detection. However, it also leads to an increased risk of false vehicle detections. For instance, in environments with a high point cloud density, the vehicle detection algorithm may identify multiple point clusters belonging to the same car, resulting in two or more bounding boxes being assigned to a single vehicle. Tracking algorithms, in addition to detection, can help reduce the number of false positives compared to detection alone.

The number of points thresholds for identifying a car object can serve as an input parameter for the vehicle detection algorithm and can be adjusted based on the characteristics of the sensor model being employed. Moreover, the processing cost of point clouds is closely tied to the point density. The point density value is also influenced by the scanning distance, as shown in Figure 18. Specifically, the spacing between laser point circles increases as the distance from the sensor grows. In the simulation pipeline, the minimum threshold number of points is selected based on the desired maximum scan distance that one intends to achieve.

- *Added artificial Gaussian noise*

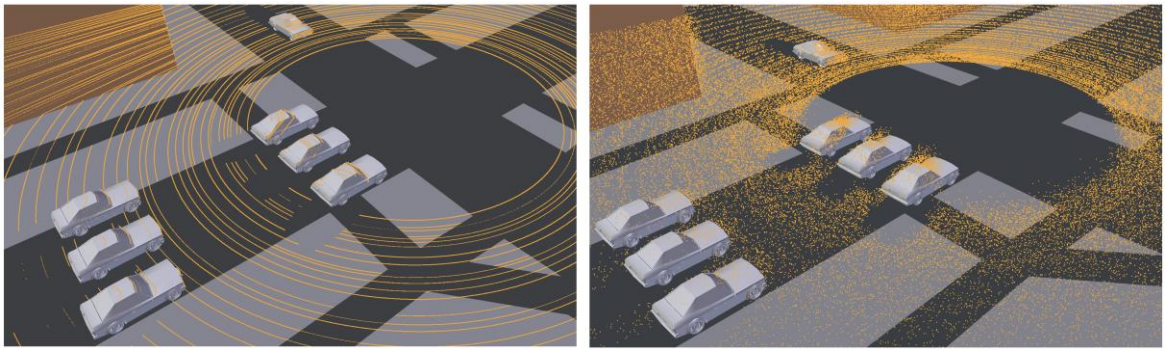

Figure 17: Point cloud visualization with zero noise (left) and added Gaussian noise (right).

In practical scenarios involving actual LiDAR systems, noise is an inherent factor that needs to be considered. Consequently, the simulation pipeline incorporates a methodology to introduce noise into the generated point cloud data. The Blensor API, for instance, allows for the specification of the noise type to be added. In this case, Gaussian noise is applied to the point cloud data (Figure 17). The inclusion of such noise in the simulation pipeline enhances the realism of the environment, thus enabling the vehicle detection algorithm to be better equipped for deployment in real-world settings.

- *Maximum scan radius*

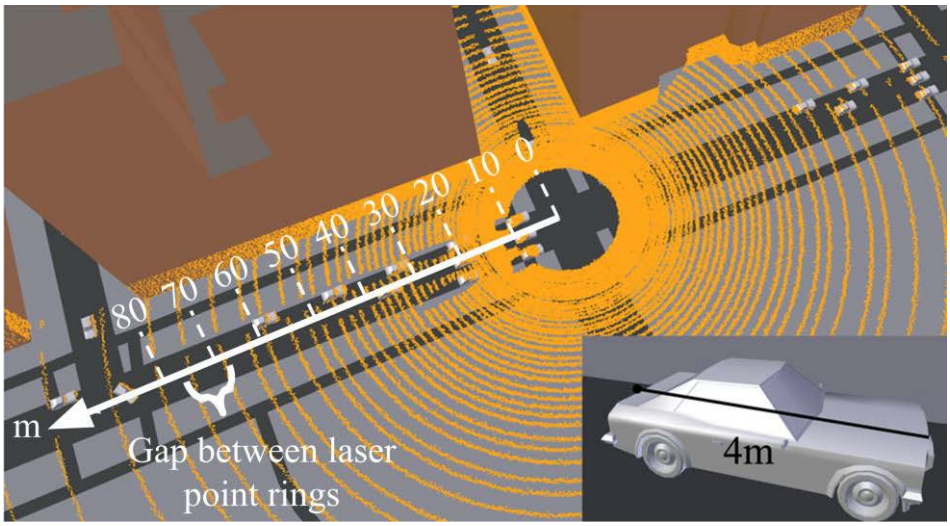

Figure 18: Scale of point cloud.

In the simulated point clouds generated by Blensor, there is an observed increase in the gap between point cloud rings as the scan radius expands (Figure 18). This phenomenon poses a challenge as it can potentially lead to the omission of vehicles from the point cloud data. Consequently, the detection accuracy of the vehicle detection algorithm tends to decrease with an increase in the LiDAR scan range. Additionally, the number of points on a detected object decreases as the LiDAR scan distance increases, resulting in an elevated false negative count for the vehicle detection algorithm.

To address this issue, the simulation pipeline incorporates a variable that represents the minimum number of LiDAR points required to identify a vehicle. The value assigned to this

variable is determined based on the average number of points found on top of a vehicle within a 75 m scan radius. Notably, it has been observed from the error model that beyond a scan distance of 75 m, the detection algorithm experiences a significant reduction in accuracy.

These considerations regarding the scan range and the corresponding impact on detection accuracy are important in optimizing the performance of the vehicle detection algorithm in practical LiDAR-based systems.

4.2 Results from the error model

The error model explained in section 3.5 is used to generate the following results.

In Figure 19, 3D coordinates from physics engine, vehicle detection algorithm and error modelling algorithm are shown in a 2D plane. In the developed simulation framework user can condition the TP, FP and FN counts to acquire desire visualization. For example, conditions can include FP $\leq$ 3 and FN $\leq$ 3, then the visualization part of the error modelling algorithm outputs corresponding visualizations related to given conditions while going through each point cloud frame of the dynamic environment.

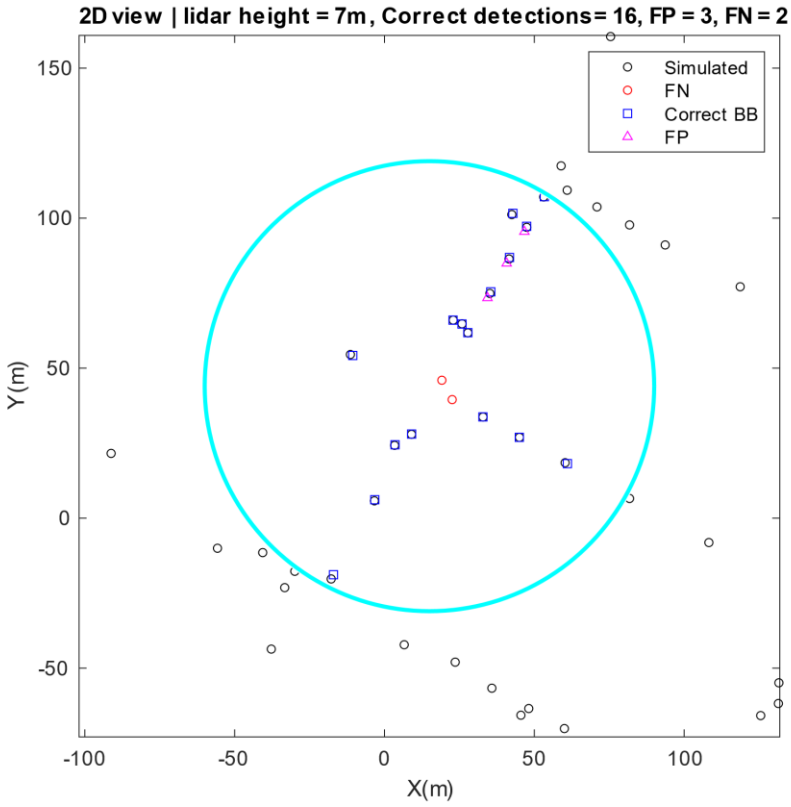

Figure 19: 2D visualization of results from error model (Circle boundary represents the LiDAR range and points are vehicles).

Different vehicle detection and tracking algorithms might have various parameters like cluster size, minimum segmentation distance between two clusters, maximum/minimum 3D coordinates to define ROI of the point cloud to consider, etc. Therefore, the objective of having this visualization output is to fine tune parameters of vehicle detection algorithm and achieve better detection accuracy.

Another output from the error model is Euclidean distance error histogram. It provides a number of instances against error difference between physics generated vehicle locations and bounding box detected locations. Histogram is plotted to get an idea how error variation scattered throughout the TP detections. Figure 20 corresponds to the [38] geometric based vehicle detection algorithm.

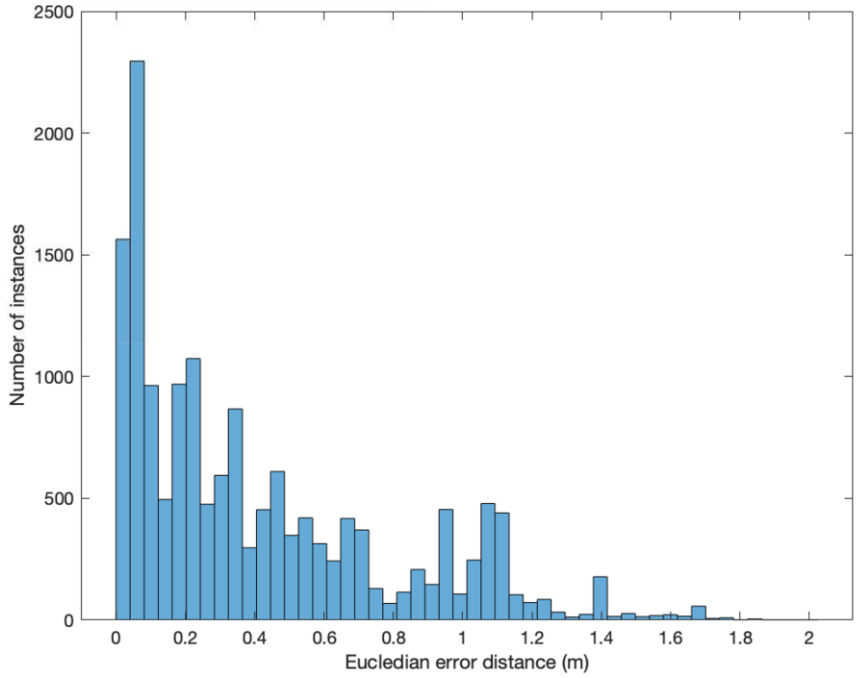

Figure 20: Histogram of bounding box distance error for LiDAR height 8m.

The histogram (Figure 20) is left skewed as expected, indicating that quality of the vehicle detection accuracy is higher. Approximately a maximum of 1.9 m, and average of 0.26 m of detection error was recorded for a simulation traffic environment with a maximum car speed of 30 Kmph. 96% of detections have an error of less than 1 m for this LiDAR configuration in Figure 20. Detection accuracy is one of quantitative output from the error model which is 83% for the LiDAR height of 8 m with a LiDAR range up to 70 m. This is given by the following equation,

$$Detection\ accuracy = \frac{TP + TN}{TP + FP + FN + TN} \tag{4.1}$$

This is the ratio between the number of correctly detected vehicles with a less than 1 m Euclidean error distance and the total number of physics generated vehicle locations. Here, the True Negatives (TN) are zero, because vehicles that are not recorded from physics engine being detected are zero.

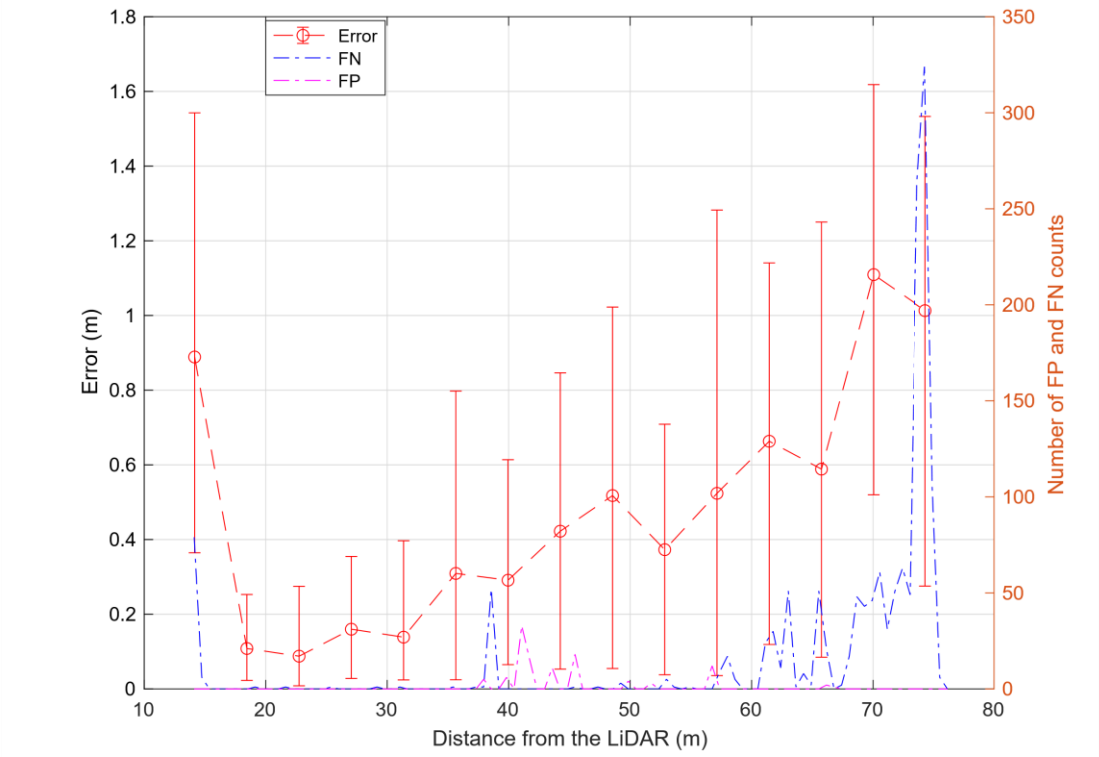

Figure 21: Bounding box detection error bar with 95% confidence interval, False Negative and False Positive counts with LiDAR range. LiDAR height is 8m.

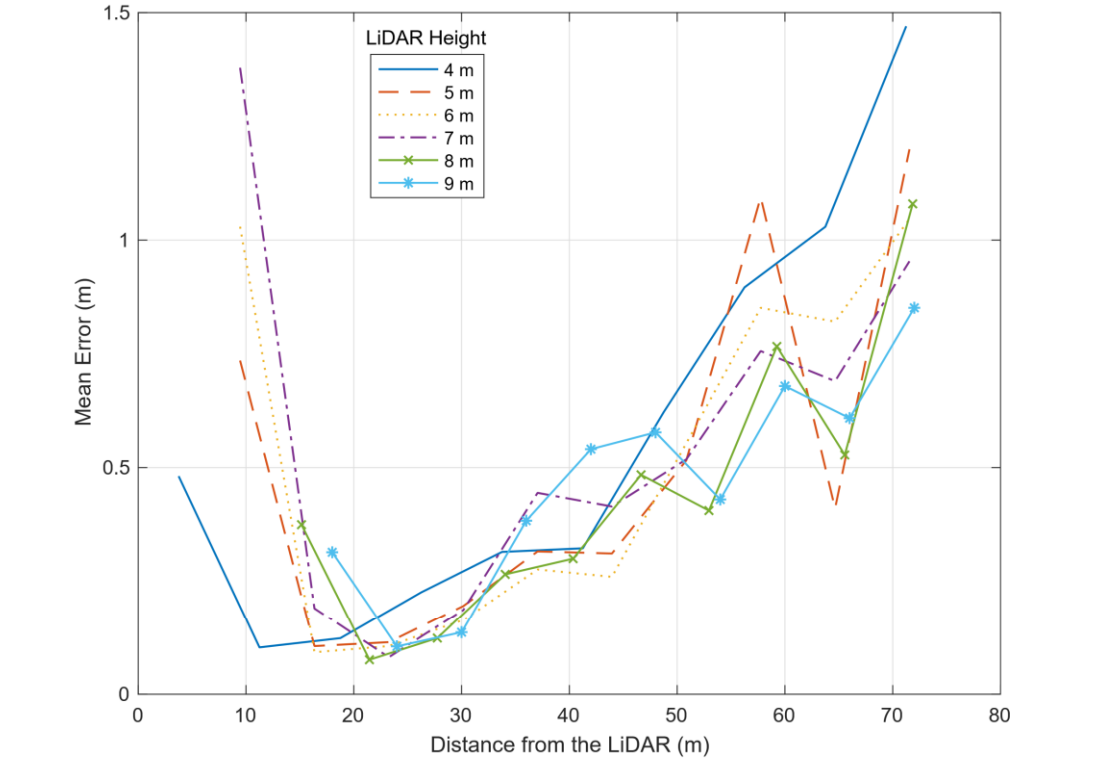

Figure 22: Bounding box detection mean error variation with LiDAR range for multiple LiDAR heights.

In the initial distance from the LiDAR, there are no error values due to the blind spot created by the LiDAR. The mean and variation of Euclidean error distance reduces up to some point and increases with the distance from the sensor (Figure 21). This phenomenon is due to having low laser point density from near the blind spot range as well as from further away from the sensor. Hence the vehicle detection algorithm will struggle to detect the vehicle in those ranges. Minimum error distance can be observed in the range of 12 to 26 m for LiDAR heights between 4 to 10 m. The minimum error distance observable area shifts to higher values of ranges as LiDAR height increases as in Figure 22. As LiDAR height increases, the mean error variation will have a higher value compared to lower LiDAR heights, but average detection accuracy increases from 4m up to 6m LiDAR sensor height and then decrease for higher sensor heights.

The LiDAR range, up to 70 m (not considering high false negatives happen at the LiDAR boundary region) has approximately 9.8% false negatives. Also, less than 1% of false positives are observed for 8 m LiDAR height.

False negative count largely increases due to shadowing in the point cloud created by the neighboring vehicles. Therefore, a false negative count does not have an incremental relationship with the sensor range, rather it shows spikes in junctions where vehicles stack up in traffic. Also, point clouds do not contain many laser points at the LiDAR boundary region (70 to 75 m). Hence detection algorithm couldn't identify those vehicles resulting in extremely high false negative counts in the boundary areas.

False positive vehicle detection happens when the detection algorithm hyperparameter corresponds to a minimum number of laser points to identify a vehicle become low. On the contrary, the high value of a minimum number of laser points to identify a vehicle will result in false negatives. Therefore, this detection algorithm parameter needs to be fine-tuned according to the environment. It is important to point out that more general and smooth graphs can be obtained by increasing the detection data points in Figure 21 and Figure 22.

These results from the error model help identify the performance of vehicle detection algorithm and LiDAR behavior in vehicular scenarios using the simulation pipeline. Pipeline is created such that user can change most of parameters (LiDAR height range to consider, LiDAR detection range, Number of detection points, confidence interval of error box plots, etc.) to get relevant information.

4.3 Periodic beam index map

The findings from a novel approach aimed at reducing Synchronization Signal Blocks (SSBs) in V2I communication are discussed.

SSBs are periodic signals transmitted by BS in cellular networks to provide timing and synchronization information to mobile devices. When a UE enters an area covered by a cellular network, it needs to perform initial synchronization with the network to establish a connection. SSBs help facilitate this synchronization process.

But consider a high mobility environment like in vehicular communication network. By having more pencil like MIMO beamforming towards the UE reduces the number of SSBs that needed to send by the base station to initialize the channel, which ultimately reduces the wireless communication overhead of the system.

To overcome that challenge, LiDAR assisted precoder based beamforming method with a periodic beam index map is introduced. Considered traffic environment from the simulation pipeline is transferred into Wireless Insite. Road area is considered as a grid of receivers (as in

Figure 23) and simulation of the wireless channels between each grid and BS has been done to get the channel matrices (H).

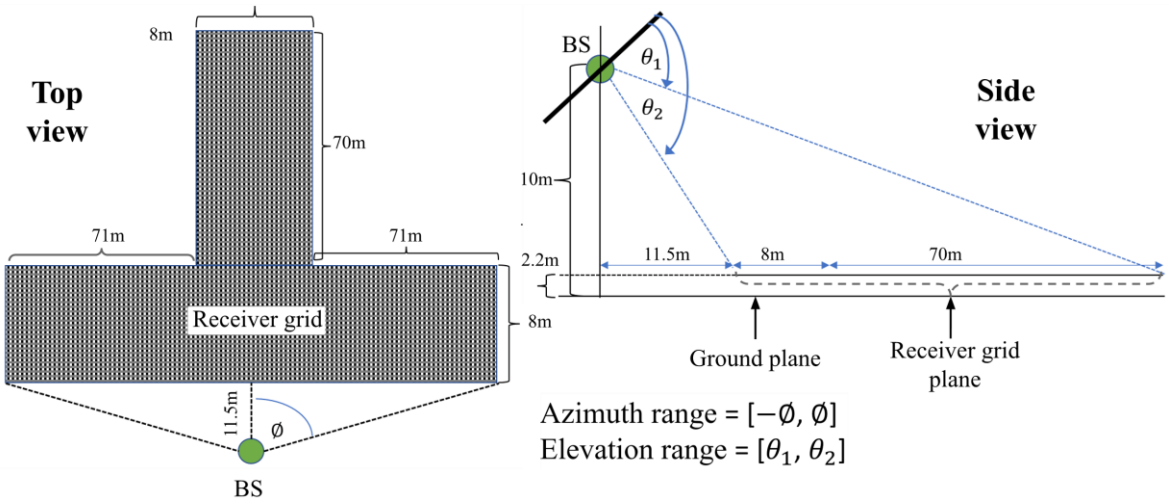

Figure 23: Top and side views of beam index map for the environment selected in section 3.1.

Getting smaller grid spacing for the beam index map is always beneficial to pinpoint the exact location of the receiver beam but 0.5m grid spacing is used to reduce the high computational overhead.

Channel matrices and precoder weights calculated according to section 3.6 with Eq.(3.9) for the weight vectors (w). Then corresponding elevation and azimuth value related to maximum RSRP for each receiver is obtained as follows,

$$RSRP = 10 \cdot log_{10}(|H^T \cdot w|^2) \tag{4.2}$$

where H denotes the channel matrix.

Now, we have elevation and azimuth angle maps with values for each receiver on the grid. Then for this particular environment with 8x8 MIMO BS, beams are discretized to 15 beams which corresponds to 3 elevation and 5 azimuth angles within the elevation range from 90° to 100° and azimuth range of -60° to 60°.

The color plot, for both elevation and azimuth beam map is used to get the beam regions. This color plots beam boundary region detection has been done using Support Vector Machine (SVM) algorithm and counter plot as in Figure 24.

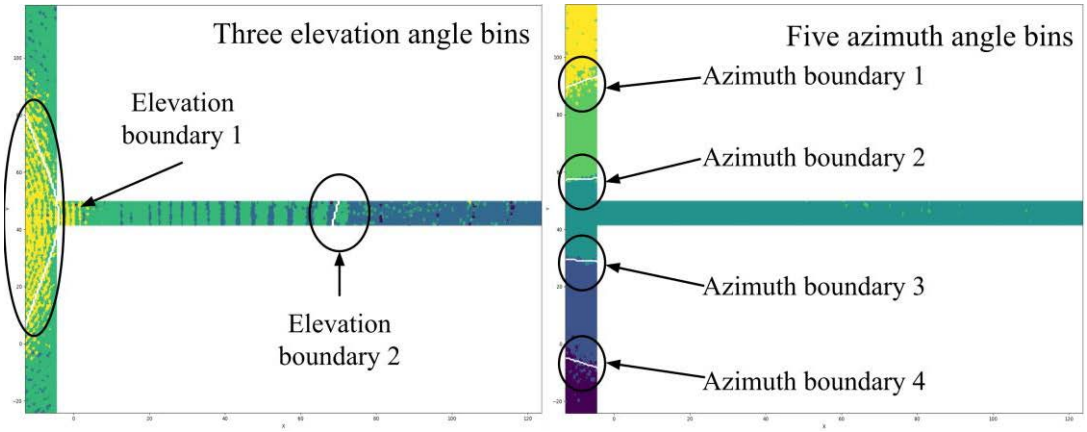

Figure 24: Resulting boundary areas for elevation and azimuth angle maps using SVM boundary detection.

The pipeline parameters can change to consider specific antenna with a given number of beams. The beam index map can be used as a lookup table to steer the beam according to the vehicle detection data, for V2I communication which reduces the additional overhead of figuring out the correct beam index with the cost of detecting accurate boundaries. This cost can be determined according to Eq. (4.3). The cost value is between 0 and 1 with 0 representing perfect boundary areas while 1 represents the maximum error of getting beam indexes.

$$cost = 1 - \left(\frac{A_\theta + A_\phi}{2}\right) \tag{4.3}$$

where A_θ and A_ϕ denote the SVM classification accuracy for elevation and azimuth maps, respectively. For this environment A_θ = 0.82 and A_ϕ = 0.97 which gives a boundary detection cost of 0.105.

The map acts like a lookup table where you provide the location of the vehicle as input from the simulation pipeline and the output will be the corresponding elevation and azimuth angle. The accuracy of the output corresponds with the SVM boundary detection accuracy. This lookup table is used for a particular time period which is determined according to the scene changes, and it can be updated according to a given period. With this method, it is not necessary to do the wireless beamforming for each instance for every vehicle which reduces the communication overhead. Furthermore, it will reduce the number of SSBs that need to be sent.

5 CONCLUSION

In B5G and 6G future networks, the complexity of networks is increasing due to diverse requirements and additional components. The development of ISAC has gained significant research attention, particularly in the utilization of sensors to enhance communication. One specific area where sensing-assisted communication has been implemented is in vehicular communication. Obtaining accurate positioning information of UEs is crucial for the successful implementation of ISAC technology. Consequently, the integration of LiDAR-like sensors to explore emerging research areas such as ML and DL has become common place in current communication networks. However, researchers require large datasets and simulation frameworks with controllable parameters to effectively evaluate these theories.

Therefore, this study undertakes an extensive literature review to identify the key components of sensing-assisted communication, focusing on LiDAR as the primary sensing agent. It elucidates the significance of ISAC in future networks, examines the applications supported by ISAC, compares various sensors for vehicular communication, highlights the importance of simulation frameworks in vehicular traffic scenarios, and presents potential vehicle detection algorithms that can be tested using a simulation framework and custom error model. Furthermore, the study explores the existing literature on intelligent beamforming in vehicular traffic environments.

The proposed simulation pipeline comprises five main stages, as depicted in Figure 6. This pipeline facilitates the generation of datasets for diverse applications, including ML, DL tasks, and optimization-based problems such as determining the optimal installation location for a LiDAR sensor in a specific environment. A custom error model algorithm is employed to identify true positive detections made by a vehicle detection algorithm using point cloud data. Additionally, the algorithm outputs the number of undetected and incorrectly detected vehicles. The visualization section of the algorithm provides insights into the variation of detection algorithm errors with respect to LiDAR range, the impact of controllable parameters, and the fluctuations in false positive and false negative detections across different configurations.

Lastly, a novel method for reducing wireless communication overhead is proposed in the context of vehicular traffic scenarios. This method employs a periodic beam index map to determine MIMO beam parameters for a specific vehicle at a given time, obviating the need for constant beam steering. The cost value is utilized to evaluate the accuracy of azimuth and elevation boundaries classification, which ultimately provides an insight for wireless communication performance.

The results obtained from the simulation pipeline, which present LiDAR behavior in a vehicular traffic scenario, as well as the outcomes derived from the periodic beam index map, demonstrating reduced wireless overhead, are presented in results and discussion section.

In future studies, the developed simulation pipeline can be extended to simulate other scenarios, such as blockage prediction, enhancing LoS handover, channel planning, and prediction, among others.

6 REFERENCES

[1] F. Liu, Y. Cui, C. Masouros, J. Xu, T. X. Han, Y. C. Eldar and S. Buzzi, "Integrated Sensing and Communications: Toward Dual-Functional Wireless Networks for 6G and Beyond," *IEEE Journal on Selected Areas in Communications,* vol. 40, pp. 1728-1767, 2022.

[2] A. Zhang, M. L. Rahman, X. Huang, Y. J. Guo, S. Chen and R. W. Heath, "Perceptive Mobile Networks: Cellular Networks with Radio Vision via Joint Communication and Radar Sensing," *IEEE Vehicular Technology Magazine,* vol. 16, pp. 20-30, 2021.

[3] H. Huang, S. Guo, G. Gui, Z. Yang, J. Zhang, H. Sari and F. Adachi, "Deep Learning for Physical-Layer 5G Wireless Techniques: Opportunities, Challenges and Solutions," *IEEE Wireless Communications,* vol. 27, pp. 214-222, 2020.

[4] C. Zhang, P. Patras and H. Haddadi, "Deep Learning in Mobile and Wireless Networking: A Survey," *IEEE Communications Surveys & Tutorials,* vol. 21, pp. 2224-2287, 2019.

[5] H. Wu, R. Hou and B. Sun, "Location Information Assisted mmWave Hybrid Beamforming Scheme for 5G-Enabled UAVs," in *ICC 2020 - 2020 IEEE International Conference on Communications (ICC)*, 2020.

[6] F. Liu, W. Yuan, C. Masouros and J. Yuan, "Radar-Assisted Predictive Beamforming for Vehicular Links: Communication Served by Sensing," *IEEE Transactions on Wireless Communications,* vol. 19, pp. 7704-7719, 2020.

[7] E. Farsimadan, F. Palmieri, L. Moradi, D. Conte and B. Paternoster, "Vehicle-to-Everything (V2X) Communication Scenarios for Vehicular Ad-hoc Networking (VANET): An Overview," in *Computational Science and Its Applications – ICCSA 2021*, Cham, 2021.

[8] A. Klautau, P. Batista, N. González-Prelcic, Y. Wang and R. W. Heath, "5G MIMO Data for Machine Learning: Application to Beam-Selection Using Deep Learning," in *2018 Information Theory and Applications Workshop (ITA)*, 2018.

[9] M. Alrabeiah, A. Hredzak, Z. Liu and A. Alkhateeb, *ViWi: A Deep Learning Dataset Framework for Vision-Aided Wireless Communications,* 2020.

[10] A. Klautau, N. González-Prelcic and R. W. Heath, "LIDAR Data for Deep Learning-Based mmWave Beam-Selection," *IEEE Wireless Communications Letters,* vol. 8, pp. 909-912, 2019.

[11] C. De Lima, D. Belot, R. Berkvens, A. Bourdoux, D. Dardari, M. Guillaud, M. Isomursu, E.-S. Lohan, Y. Miao, A. N. Barreto, M. R. K. Aziz, J. Saloranta, T. Sanguanpuak, H. Sarieddeen, G. Seco-Granados, J. Suutala, T. Svensson, M. Valkama, B. Van Liempd and H. Wymeersch, "Convergent Communication, Sensing and Localization in 6G Systems: An Overview of Technologies, Opportunities and Challenges," *IEEE Access,* vol. 9, pp. 26902-26925, 2021.

[12] A. Oliveira, F. Bastos, I. Trindade, W. Frazao, A. Nascimento, D. Gomes, F. M_ller and A. Klautau, "Simulation of machine learning-based 6G systems in virtual worlds," *ITU Journal on Future and Evolving Technologies,* vol. 2, p. 113–123, August 2021.

[13] A. Oliveira and T. Vazão, "Generating Synthetic Datasets for Mobile Wireless Networks with SUMO," in *Proceedings of the 19th ACM International Symposium on Mobility Management and Wireless Access*, New York, NY, USA, 2021.

[14] A. Ali, N. González-Prelcic, R. W. H. J. au2 and A. Ghosh, *Leveraging Sensing at the Infrastructure for mmWave Communication,* 2019.

[15] C. Sturm and W. Wiesbeck, "Waveform Design and Signal Processing Aspects for Fusion of Wireless Communications and Radar Sensing," *Proceedings of the IEEE,* vol. 99, pp. 1236-1259, 2011.

[16] P. Kumari, A. Mezghani and R. W. Heath, "JCR70: A Low-Complexity Millimeter-Wave Proof-of-Concept Platform for a Fully Digital SIMO Joint Communication-Radar," *IEEE Open Journal of Vehicular Technology,* vol. 2, pp. 218-234, 2021.

[17] F. Liu, C. Masouros, A. P. Petropulu, H. Griffiths and L. Hanzo, "Joint Radar and Communication Design: Applications, State-of-the-Art, and the Road Ahead," *IEEE Transactions on Communications,* vol. 68, pp. 3834-3862, 2020.

[18] H. Griffiths, "The MAMMUT Phased Array Radar: Compulsive Hoarding," in *2019 International Radar Conference (RADAR)*, 2019.

[19] B. Li and A. P. Petropulu, "Joint Transmit Designs for Coexistence of MIMO Wireless Communications and Sparse Sensing Radars in Clutter," vol. 53, pp. 2846-2864, 2017.

[20] J. Li and P. Stoica, "MIMO Radar with Colocated Antennas," *IEEE Signal Processing Magazine,* vol. 24, pp. 106-114, 2007.

[21] M. Roberton and E. R. Brown, "Integrated radar and communications based on chirped spread-spectrum techniques," in *IEEE MTT-S International Microwave Symposium Digest, 2003*, 2003.

[22] Y. Cui, F. Liu, X. Jing and J. Mu, "Integrating Sensing and Communications for Ubiquitous IoT: Applications, Trends, and Challenges," *IEEE Network,* vol. 35, pp. 158-167, 2021.

[23] C. Ouyang, Y. Liu and H. Yang, "Performance of Downlink and Uplink Integrated Sensing and Communications (ISAC) Systems," *IEEE Wireless Communications Letters,* vol. 11, pp. 1850-1854, 2022.

[24] Q. Qi, X. Chen, A. Khalili, C. Zhong, Z. Zhang and D. W. K. Ng, "Integrating Sensing, Computing, and Communication in 6G Wireless Networks: Design and Optimization," *IEEE Transactions on Communications,* vol. 70, pp. 6212-6227, 2022.

[25] X. Liu, H. Zhang, K. Long, M. Zhou, Y. Li and H. V. Poor, "Proximal Policy Optimization-Based Transmit Beamforming and Phase-Shift Design in an IRS-Aided ISAC System for the THz Band," *IEEE Journal on Selected Areas in Communications,* vol. 40, pp. 2056-2069, 2022.

[26] T. Zhang, K. Zhu, S. Zheng, D. Niyato and N. C. Luong, "Trajectory Design and Power Control for Joint Radar and Communication Enabled Multi-UAV Cooperative Detection Systems," *IEEE Transactions on Communications,* vol. 71, pp. 158-172, 2023.

[27] P. Liu, G. Zhu, W. Jiang, W. Luo, J. Xu and S. Cui, "Vertical Federated Edge Learning with Distributed Integrated Sensing and Communication," *IEEE Communications Letters,* vol. 26, pp. 2091-2095, 2022.

[28] N. Huang, T. Wang, Y. Wu, Q. Wu and T. Q. S. Quek, "Integrated Sensing and Communication Assisted Mobile Edge Computing: An Energy-Efficient Design via Intelligent Reflecting Surface," *IEEE Wireless Communications Letters,* vol. 11, pp. 2085-2089, 2022.

[29] B. Liu, J. Liu and N. Kato, "Optimal Beamformer Design for Millimeter Wave Dual-Functional Radar-Communication Based V2X Systems," *IEEE Journal on Selected Areas in Communications,* vol. 40, pp. 2980-2993, 2022.

[30] Y. Gong, Y. Wei, Z. Feng, F. R. Yu and Y. Zhang, "Resource Allocation for Integrated Sensing and Communication in Digital Twin Enabled Internet of Vehicles," *IEEE Transactions on Vehicular Technology,* vol. 72, pp. 4510-4524, 2023.

[31] H. Wymeersch, G. Seco-Granados, G. Destino, D. Dardari and F. Tufvesson, "5G mmWave Positioning for Vehicular Networks," *IEEE Wireless Communications,* vol. 24, pp. 80-86, 2017.

[32] Z. Feng, Z. Fang, Z. Wei, X. Chen, Z. Quan and D. Ji, "Joint radar and communication: A survey," *China Communications,* vol. 17, pp. 1-27, 2020.

[33] S. Ali, W. Saad, N. Rajatheva, K. Chang, D. Steinbach, B. Sliwa, C. Wietfeld, K. Mei, H. Shiri, H.-J. Zepernick, T. M. C. Chu, I. Ahmad, J. Huusko, J. Suutala, S. Bhadauria, V. Bhatia, R. Mitra, S. Amuru, R. Abbas, B. Shao, M. Capobianco, G. Yu, M. Claes, T. Karvonen, M. Chen, M. Girnyk and H. Malik, *6G White Paper on Machine Learning in Wireless Communication Networks,* 2020.

[34] C. Liu, W. Yuan, S. Li, X. Liu, H. Li, D. W. K. Ng and Y. Li, "Learning-Based Predictive Beamforming for Integrated Sensing and Communication in Vehicular Networks," *IEEE Journal on Selected Areas in Communications,* vol. 40, pp. 2317-2334, 2022.

[35] A. Alkhateeb, *DeepMIMO: A Generic Deep Learning Dataset for Millimeter Wave and Massive MIMO Applications,* 2019.

[36] Y.-G. Lim, Y. J. Cho, M. S. Sim, Y. Kim, C.-B. Chae and R. A. Valenzuela, "Map-Based Millimeter-Wave Channel Models: An Overview, Data for B5G Evaluation and Machine Learning," *IEEE Wireless Communications,* vol. 27, pp. 54-62, 2020.

[37] X. Jin, H. Yang, X. He, G. Liu, Z. Yan and Q. Wang, "Robust LiDAR-Based Vehicle Detection for On-Road Autonomous Driving," *Remote Sensing,* vol. 15, 2023.

[38] *Track Vehicles Using Lidar: From Point Cloud to Track List - MATLAB & Simulink – MathWorks*

[39] Y. Zhou and O. Tuzel, "VoxelNet: End-to-End Learning for Point Cloud Based 3D Object Detection," in *2018 IEEE/CVF Conference on Computer Vision and Pattern Recognition*, 2018.

[40] A. Paigwar, O. Erkent, C. Wolf and C. Laugier, "Attentional PointNet for 3D-Object Detection in Point Clouds," in *2019 IEEE/CVF Conference on Computer Vision and Pattern Recognition Workshops (CVPRW)*, 2019.

[41] R. O. Chavez-Garcia and O. Aycard, "Multiple Sensor Fusion and Classification for Moving Object Detection and Tracking," *IEEE Transactions on Intelligent Transportation Systems,* vol. 17, pp. 525-534, 2016.

[42] X. Zhao, P. Sun, Z. Xu, H. Min and H. Yu, "Fusion of 3D LIDAR and Camera Data for Object Detection in Autonomous Vehicle Applications," *IEEE Sensors Journal,* vol. 20, pp. 4901-4913, 2020.

[43] *ETSI TR 138 913 V14.3.0. 5G; Study in scenarios and requirements for next-generation access technologies.*

[44] *Openstreetmap, this package includes static environment data such as roads, buildings, and traffic lights.*

[45] P. A. Lopez, M. Behrisch, L. Bieker-Walz, J. Erdmann, Y.-P. Flötteröd, R. Hilbrich, L. Lücken, J. Rummel, P. Wagner and E. Wießner, "Microscopic Traffic Simulation using SUMO," in *the 21st IEEE International Conference on Intelligent Transportation Systems*, 2018.

[46] M. Gschwandtner, R. Kwitt, A. Uhl and W. Pree, "BlenSor: Blender Sensor Simulation Toolbox," in *Advances in Visual Computing*, Berlin, 2011.

[47] *Blender Python API — docs.blender.org*

[48] L. Wen, L. He and Z. Gao, "Research on 3D Point Cloud De-Distortion Algorithm and Its Application on Euclidean Clustering," *IEEE Access,* vol. 7, pp. 86041-86053, 2019.

[49] *ETSI TR 37.840 Study of Radio Frequency (RF) and Electromagnetic Compatibility (EMC) requirements for Active Antenna Array System (AAS) base station.*